Dear reviewer #1,

Thanks very much for the precious comments and suggestions. All the comments and suggestions are addressed in the revised manuscript.

1. With respect to constraints on the overall PI global emissions of N_2O, I have more confidence in the top-down approach using atmospheric concentrations and lifetimes of N_2O, than the bottom up simulations of a highly parameterized process model. The most recent top-down estimate (Prather et al., 2015) is cited in passing by the authors, but the estimates are not included in the present manuscript. The estimates from the IPCC AR4 and from Davidson & Kanter (2014), mentioned in lines 53-54, were based largely on the 2012 paper by Prather et al., but their 2015 paper provides an important update on lifetime estimates and resulting PI emission estimates. They now recommend using lifetimes of 123 years for PI and 116 years for the present (+/- 9 years), and from those lifetime estimates, they derive a new PI emission estimate of 10.5 Tg/yr. Fortunately, this is very close to other estimates, including the one from this study. Nevertheless, it should be specifically cited.

Response:

We have cited the recent study by Prather et al. (2015) in the introduction and discussion sections of the revised manuscript.

Line 55-57: Prather et al. (2015) provided an estimate of the pre-industrial emissions (total natural emission: 10.5 Tg N yr^{-1}) based on the most recent study with a corrected lifetime of 116 years.

Line 267-275: "Top-down" methodology used to estimate N_2O emissions is based on atmospheric measurements and an inversion model (Thompson et al. 2014). Prather et al. (2012) provided an estimate of 9.1±1.0 Tg N yr^{-1} of natural emission in the pre-industrial era using observed pre-industrial abundances of 270 ppb and model estimates of lifetime decreased from 142 years in the pre-industrial era to 131±10 years in the present-day. Later, Prather et al. (2015) re-evaluated N_2O lifetime based on Microwave Limb Sounder satellite measurements of stratospheric, which was consistent with modeled values in the present-day. The lifetime in the pre-industrial era and present-day was estimated to be 123 and 116±9 years, respectively. The current lifetime increases the pre-industrial natural emission from 9.1±1.0 to 10.5 Tg N yr^{-1}.

2. The point that the lifetime has probably decreased since PI times should be discussed. As far as I can tell, a varying lifetime cannot be incorporated into the one-box model (line 171) used by the authors. Perhaps the resulting global estimate is not terribly sensitive to this change, but that should be evaluated and discussed.

Response:

In the revised version, we have removed the one-box model validation. In addition, we added the discussion of the decreased lifetime since PI times, which was also mentioned in the response to question #1 (Line 267-275).

3. I fail to see how the analysis presented in Figure 7 and Table 1 provides additional confidence in the summed global estimate from this study. I can see the value of a sensitivity analysis of initial PI atmospheric concentrations and lifetimes, which Prather's papers have already done and for which they could be cited. In contrast, the analysis in Fig. 7 and Table 1 is clouded by the unclear source of annual emissions over the simulated time period and the validity of those assumptions. The text (lines 182- 185) suggests that model output was used for annual emission estimates: "The mean with 95% confidence intervals, the maximum, and minimum values of estimates from DLEM simulations were applied as initial emissions to calculate the atmospheric N_2O concentration in 2006 as shown in Table 1 (Scenarios 1–4 and baseline), as well as concentration changes from 1860 to 2006, as shown in Figure 7." However, the Fig. 7 captions indicates that the "net additions of anthropogenic N_2O emission amount in different years were listed in Syakila and Kroeze, 2011." I don't understand which was used to estimate annual increments of N_2O concentration in Fig 7 – was it model output, as indicated on lines 182-185, or was it the net additions estimated by S&K as indicated in the figure caption? Both have problems. S&K estimated fairly substantial N_2O emissions from agriculture during the late 19th
and early 20th centuries, but they also estimated a rather large decrease in natural emissions compared to 1500 (which are very difficult to estimate, see my further comments below), so their estimate of the net change relative to 1500 was small for this time period. However, the starting point for the present study is 1860. Therefore, it is incorrect to subtract this decline in natural emissions that preceded 1860 from the growth in anthropogenic emissions since 1860. S&K did this to show changes since their starting point of 1500, but using their "net additions" column

without accounting for a different starting point in the present study introduces a significant bias. It is the net change relative to 1860 that is important for the present study, so the "net additions" estimated by S&K should be recalculated relative to 1860 if they are to be used in the analysis for Table 1 and Fig. 7.

I showed in my 2009 paper, and Smith et al. (2012) have affirmed, that atmospheric N_2O began rising significantly many decades before fertilizer use became common in the 1950s, and so the "net additions" to the atmosphere must have been larger than those estimated by S&K relative to 1500, although they may be similar if they were corrected to be relative to 1860. We speculate that this increase in emissions between 1860 and 1950 was due to mineralization of soil N as agriculture expanded into regions of previously untilled soils, thus mobilizing N for rapid cycling, including a fraction lost at N_2O. I also suspect that the current DLEM may not include effects of soil mining when virgin soil is first tilled, so if Table 1 is based on DLEM simulations, as indicated in the text on lines 182-185, then I suspect emissions from 1860 to 1950 were underestimated, which would affect the slope of the trend line later in the analysis as well.

I realize that the point of Figure 7 is not the accuracy of the simulated trend line, but rather the end point, but if the trend line agrees so poorly with the observations, then one has to question the validity of the model and the input data, which calls into question the reliability of the end point analysis. I believe that Fig. 7 and Table 1 could be replaced with citations of the sensitivity analyses done by Prather et al. (2012, 2015), but if the authors persist in wanting to include their own analysis, I would suggest that they utilize another source of "net addition" emissions than those of S&K relative to 1500.

Response:

According to your suggestions, we have removed the one-box model validation. Instead, we cited the work done by Prather et al. (2012, 2015) and compared our results with theirs in the section 3.2.

Line 276–287: Natural sources for N_2O include soil under natural vegetation, oceans, and atmospheric chemistry (Ciais et al., 2014). The emission from atmospheric chemistry was estimated as 0.6 with an uncertainty range of 0.3–1.2 Tg N yr^{-1}. Syakila and Kroeze (2011) estimated global natural emissions from oceans as 3.5 Tg N yr^{-1}. Oceanic emission was estimated as 3.8 with an uncertainty range of 1.8–5.8 Tg N yr^{-1} in the IPCC AR4. However, the uncertainty range became larger (1.8–9.4 Tg N yr^{-1}) in the IPCC AR5. In our study, the simulated N_2O

emission was from agricultural and natural soils. The natural emission was estimated as 5.78 (4.4–7.72) Tg N yr^{-1}. Combining the atmospheric chemistry and the ocean emissions in the IPCC AR5 with the natural emissions from our study, the global total natural N_2O emissions were 10.18 (6.5-18.32) Tg N yr^{-1}. The large uncertainty range was attributed to the uncertainty from oceanic emission, atmospheric chemistry emission, and our estimation. The estimated global total amount (10.18 Tg N yr^{-1}) in this study was comparable to the estimate (10.5 Tg N yr^{-1}) by Prather et al. (2015) using the top-down approach.

4. The change in "natural" emissions before and after 1860 should be discussed. As I noted above, S&K deduce a substantial decline in natural emissions from 1500 to 1850. Similarly, I included a significant change in non-agricultural soil emissions due to tropical deforestation, which began growing rapidly in the late 20th century (Davidson 2009). Whether pre-1850 or post-1950, these changes in natural soil emissions are difficult to estimate, but the uncertainties that they represent should be considered, and biases resulting from how they are or are not included should be considered.

Response:

We agree that different factors caused different variation patterns in N_2O fluxes before and after 1860. We did not consider the pre-1850 natural emission change because we assumed emission in 1860 can represent the pre-industrial level although it has declined from 1500 to 1850. Our estimation from the process-based model can capture the N_2O emission due to land use change in the late 20^{th} century, but it is beyond the scope of this paper. Since pre-industrial N_2O emission is not always stable and remains a large uncertainty, our estimation can only go back to 1860 and represent N_2O level before intensive human disturbance.

5. While the top-down approach of Prather et al. (2012, 2015) and the one box model used in the present study help constrain total PI emissions, the soil emission estimate must still be made by difference between total emissions and oceanic emissions. While the AR5 estimate of 3.8 Tg N_2O-N/yr (range: 1.8 - 9.4; Ciais et al., 2013) is widely cited for emissions from the oceans, it is highly uncertain, so simply subtracting 3.8 (or 3.5 – 4.5 as in Table 1 of the present manuscript) from a total PI source estimate of about 11 Tg N_2O-N/yr (+/-1) doesn't really narrow the confidence estimate of the PI terrestrial source a great deal. Indeed, I just discovered a curious inconsistency

between the AR5 best estimate of 3.8 with a review paper by Voss et al. (2013), which cites that same 3.8 value for N_2O emissions from the open ocean, but then adds another 1.7 Tg N_2O-N/yr for emissions from the continental shelf regions. I don't know if the AR5 review of the literature failed to adequately represent continental shelf regions or if Voss et al. might be double accounting. If Voss et al. are correct, the AR5 estimate of oceanic emissions may be biased toward the low end, which would mean that the terrestrial PI source may more likely be in the range of 5 Tg N_2O-N/yr or less. In any case, this highlights how uncertain the oceanic estimate is, which means we have to have similar uncertainty in the estimate of the PI terrestrial source. The narrow range of uncertainty in the present study's PI terrestrial source (6.03–6.36 Tg N_2O-N/yr) reported on line 331 is unrealistically small.

Response:

Yes, the soil emission estimation must still be made by difference between total emissions and oceanic emissions regardless of methodology (top-down or bottom-up). In the IPCC AR5, the average oceanic emission is 3.8 Tg N yr^{-1}, with a larger uncertainty range compared with the estimate in the AR4. The estimate from Voss et al. (2013) indicated that oceanic emission was 1.7 Tg N yr^{-1} more than the average in the AR5. It is because they considered the emissions (1.7 Tg N yr^{-1}) from "rivers, estuaries, and coastal zones" as the marine emissions, as written in Table 7.7 of the IPCC AR4 Chapter 7. Thus, the average estimation in AR5 is still trustable. In this study, to compare with the results (10.5 Tg N yr^{-1}) in Prather et al. (2015), we need to sum our estimate and other natural emissions. The global total natural N_2O emissions were 10.18 (6.5-18.32) Tg N yr^{-1} in the preindustrial era.

The small uncertainty range shown in the upper panel of Fig. 5 was the 95% confidence interval of the mean estimate, as explained in the manuscript. The uncertainty range of pre-industrial N_2O emissions was present using the minimum and maximum estimate (4.76–8.13 Tg N yr^{-1}) in this study, which was consistent with other studies, such as the reported estimates in the IPCC AR5. Here, the Bootstrap resampling method was used to define the uncertainty bounds of global mean N_2O emission (6.20 Tg N yr^{-1}) (shown in line 216-219 of previous manuscript). It was used to verify the stability of the LHS approach. The 95% confidence intervals (6.03-6.36 Tg N yr^{-1}) of the mean did not represent the uncertainty range for pre-industrial N_2O emission in this study. Thus, we will not report this narrow range in the revised manuscript to avoid the confusion.

6. The authors have misunderstood the emission estimates from my 2009 paper, which they incorrectly describe on lines 299-301: "However, the indirect emissions from the riverine induced by the leaching and runoff of manure applications in agro-ecosystems, legume crop N fixation, and human sewage discharging have not been addressed in Davidson (2009)." On the contrary, I derived emissions factors from a statistical model that was constrained by the historical record of atmospheric concentrations and fertilizer and manure use, so the emission factors derived from that analysis necessarily included all of the emissions, direct and indirect, that could be statistically correlated with historical fertilizer and manure use ("The sources attributed to fertilizers and manures include indirect emissions from downwind and downstream ecosystems, including human sewage." Davidson, 2009). Therefore, it is incorrect for the authors to calculate an additional indirect source (line 305) using IPCC default factors to add onto the estimate that they took from my paper that they misunderstood to be only direct emissions. They could either use an unmodified estimate from my paper or they could derive a new one, based on IPCC default values for both direct and indirect emissions based on estimates of BNF, fertilizer-N, and manure-N for 1860. Furthermore, note that the 0.42 Tg N_2O-N/yr that they extracted from my paper for 1860 was for anthropogenic biological emissions (i.e., soils) only, and that there were also some other anthropogenic emissions at that time, such as biomass burning (see SI for Davidson 2009).

Response:

We are sorry for the misunderstanding of this paper. We deleted this sentence and recalculated the overall N_2O emissions from this paper. In Davidson (2009), two approaches (top-down and bottom-up) had been applied to estimate the anthropogenic biogenic N_2O emissions in 1860. The estimates from top-down and bottom-up were 0.42 and 0.54 Tg N yr^{-1}, respectively. Thus, the final number we used in this study was 0.5 with an uncertainty range of 0.4–0.6 Tg N yr^{-1}. In addition, N_2O from the biomass burning was assumed to be 0.2 Tg N yr^{-1} in 1860 in Davidson (2009). In sum, the total anthropogenic N_2O emission in 1860 was estimated as 0.7 (0.6–0.8) Tg N yr^{-1} in Davidson (2009). We added below content in the revised version:

Line 332-334: The pre-industrial anthropogenic N_2O sources in his study included biomass burning, agriculture activities (e.g., manure application, and the cultivation of legume) and human sewage, the sum of which was 0.7(0.6–0.8) Tg N yr^{-1} (Davidson, 2009).

7. The authors should also acknowledge that there were anthropogenic effects on the N_2O budget before 1860, so the 1860 fluxes don't necessarily represent only "natural" emissions. This includes some N_2O from agricultural expansion that mined soil N and also added BNF, some biomass burning, a tiny amount of industrial and transportation sector emissions, and possibly a loss of emissions from degraded natural soils that had been plowed for centuries or millennia, some of which were highly eroded.

Response:

Yes, the 1860 fluxes don't necessarily represent only "natural" emissions. In our study, when we mentioned "natural" emissions, we excluded the emissions from cropland soils. Our study has only addressed the anthropogenic emissions from cropland expansion and manure application, but we are unable to simulate the anthropogenic emissions from biomass burning and other sectors. As described in the response 6, we have added the discussion on the pre-industrial anthropogenic N_2O emission in this manuscript (Section 3.4 Line 332-334).

See the section 3.4, Line 322-346:

3.4 The N_2O budget in the pre-industrial era

The observed N_2O concentration reflects the result of dynamic production and consumption processes in soils as soils act as sources or sinks of N_2O emissions through denitrification and nitrification (Chapuis-Lardy et al., 2007). There was a slight increase of atmospheric N_2O concentration during 1750–1860 according to the ice core records, but showed a rapid increase from 1860 to present (Ciais et al., 2014). Nature sources of N_2O emissions have been discussed in section 3.2 & 3.3. Previous studies found that there were some anthropogenic N_2O emissions along with the natural sources in the pre-industrial era (Davidson, 2009; Syakila and Kroeze, 2011). Syakila and Kroeze (2011) found anthropogenic N_2O emission began since 1500 because of the biomass burning and agriculture. The total anthropogenic N_2O emission in their study was estimated as 1.1 Tg N in 1850. In addition, Davidson (2009) derived a time-course analysis of sources and sinks of atmospheric N_2O since 1860. The pre-industrial anthropogenic N_2O sources in his study included biomass burning, agriculture (e.g. manure application, and the cultivation of legume) and human sewage, the sum of which was 0.7 (0.6–0.8) Tg N yr^{-1} (Davidson, 2009). Thus, anthropogenic N_2O emission has already existed in 1860, but in a small magnitude as compared with the contemporary amount.

Davidson (2009) mentioned that there was possibly a certain amount of N_2O loss in the pre-industrial period through atmospheric sink and the reduced emission from tropical deforestation. He estimated the anthropogenic sink as 0.26 Tg N in 1860. In addition, the deforestation of tropical forest might have caused a loss of N_2O emissions in 1860, which was estimated as 0.03 Tg N (Davidson, 2009). However, studies have shown that the conversion of forest to pasture and cropland could increase or have no effect on N_2O emissions because the effects depended on disturbance intensity of human activities on soil conditions (van Lent et al., 2015). For instance, N_2O emissions tended to increase during the first 5–10 years after conversion and thereafter might decrease to average upland forest or low canopy forest levels in the non-fertilized croplands and pastures. In contrast, emissions were at a high level during and after fertilization in fertilized croplands (van Lent et al., 2015). Thus, more work is needed to study how forest degradation affects N_2O fluxes (Mertz et al., 2012).

8. Although my comments above all focus on the PI global total estimate, perhaps the more important contribution of this manuscript is the simulated spatial distribution of those PI soil emissions. It is not surprising that the model simulates the majority of the soil emissions coming from tropical forest soils. That is also true today for nonagricultural soils. There are a few curious details that jump out at me from the map (Fig. 4). Why are emissions from the Amazon Basin and SE Asia so much lower than from the Congo Basin? Other models that I am aware of don't show that difference (e.g., Zhuang et al., 2012; Stehfest & Bouwman, 2006; Potter et al., 1996). Which of the datapoints in Fig. 3 are from tropical forests and which continents are they from? Is there validation support for the Congo having much higher emissions that the Amazon
or SE Asia? More discussion would be helpful to interpret the variation shown in this map, such as where agriculture was or had been, where wetlands are, and where there are hot spots other than tropical forests. For example, I see a bunch of small red spots that appear to be near the Andes range, which puzzles me, but perhaps there is a good explanation. Ditto for why Northeastern Brazil, which is generally rather xeric, shows up as a hot spot. Also curious are the hot spots in southwestern China and the southeast coast of Australia.

(1) Why are emissions from the Amazon Basin and SE Asia so much lower than from the Congo Basin? Other models that I am aware of don't show that difference (e.g., Zhuang et al., 2012; Stehfest & Bouwman, 2006; Potter et al., 1996).

Response:

There are three major explanations for the spatial pattern differences among various studies. Firstly, the vegetation map in our study includes at most five biome types (at most four natural vegetation types and one crop type) within each grid cell. For example, in the Congo and Amazon Basin, the major natural vegetation type is Tropical Broadleaf Evergreen Forest (TrBEF). Many other models only include one vegetation type within each grid cell. This difference can cause large difference in spatial distribution of N_2O emissions between our results and other model simulations.

Secondly, DLEM simulates both soil nitrogen transformation and nitrogen export or leaching into riverine ecosystems (see section 2.1). Many other models don't simulate nitrogen leaching or export. In our simulation, we found that high rainfall (especially heavy rainfall events) can cause a large amount of available nitrogen exports to riverine ecosystems and thus reduce soil available N and N_2O emissions in these grid cells.

The third cause may be the difference in model driving data. Stehfest & Bouwman (2006) used the mean annual precipitation and annual temperature developed by New et al. (1999) during 1961–1990. In Zhuang et al., (2012), they used the monthly data from the original literature and a historical climate database from the Climate Research Unit during 1961–2002 (Mitchell and Jones, 2005). While, DLEM used the long-term mean climate datasets (daily CRUNCEP climate data) from 1901–1930 to represent the initial climate state in 1860.

In the two studies mentioned above, they stated that soil and climate characteristics are major factors that affect N_2O emissions. Unfortunately, neither of them showed the spatial distribution of precipitation or temperature, and the correlation between the climate and N_2O emissions. Moreover, through comparing the spatial N_2O emission map from those studies, we found that the distributions and magnitudes of emissions in the Congo, Amazon Basin, and Southeast Asia also differed significantly.

The spatial patterns of annual precipitation and temperature in this study are shown in Fig. S3. The Congo, Amazon Basin, and Southeast Asia are located in the tropics. The three regions have similar annual temperature (Fig. S2a), but have significantly different annual precipitation (Fig. S2b). In some areas in Amazon Basin and Southeast Asia, the annual precipitation was even higher than 3000 mm. In contrast, the annual precipitation in the Congo varied from 1300 to 2000 mm. In the DLEM, we explicitly considered the daily N leaching and runoff. Because of the heavy

rainfall in the Amazon Basin and Southeast Asia, more N might be leached from the soil during the wet season, which could cause the lower annual N_2O emissions. In addition, both denitrification and nitrification are highly affected by the soil water content. As field experiments revealed N_2O or NO could be reduced into N_2 when soils are in saturation (Davidson et al., 2000), DLEM also represent the formation and proportion of N_2O in total nitrogen oxides, considering the effect of soil moisture change. Thus, excessive soil water content during the wet season in Amazon Basin and Southeast Asia might reduce the activities of microbes, thus causing smaller amount of N_2O emission.

(2) Which of the datapoints in Fig. 3 are from tropical forests and which continents are they from?

Response:

Firstly, we are sorry for the mistake in this Figure. The x-axis should be "observed N_2O emission" rather than "simulated N_2O emission". In the new version, we redraw this figure. In addition, we used different symbols to mark all sites in Fig. 3 to make it clearly show the locations of all 20 sites. The information of each site can be found in the supplementary material (Table S1).

(3) Is there validation support for the Congo having much higher emissions that the Amazon or SE Asia?

Response:

There were only two sites in the validation from southeast Asia (site 14) and the east coast of Austria (site 10). Unfortunately, there was no available validation to support the arguments that the Congo has much higher emissions than the Amazon Basin or Southeast Asia. However, we did find some measurements in Kim et al. (2016), which could support our estimates in the central Africa. In their study, they calculated the average N_2O emission from ten observations in the Congo Basin, which was 4.2±1.5 kg N ha^{-1} yr^{-1} and close to our estimates in this region.

(4) More discussion would be helpful to interpret the variation shown in this map, such as where agriculture was or had been, where wetlands are, and where there are hot spots other than tropical forests.

Response:

The spatial distributions of cropland and wetlands have been provided in the manuscript. Meanwhile, the emission from pre-industrial cropland was discussed in line 234–243. It is hardly to make sure the certain crop types 150 years ago. Thus, N_2O emission from cropland remained quite uncertain. For the N_2O emission from wetlands and peatlands, we have discussed in line 255–266. We did not include the estimate of pre-industrial wetlands or peatlands because of the uncertainty of wetland area and distribution, but it will be included in the future study. The results in the DLEM simulation indicated that where natural vegetation was, specifically the tropical forest, were hot spots for N_2O emissions in the pre-industrial period. Some scattered hot spots the reviewer mentioned were also from the tropics as described below.

(5) I see a bunch of small red spots that appear to be near the Andes range, which puzzles me, but perhaps there is a good explanation. Ditto for why Northeastern Brazil, which is generally rather xeric, shows up as a hot spot. Also curious are the hot spots in southwestern China and the southeast coast of Australia.

Response:

We have noticed those “hot spots”. Near the Andes range and in southwestern China, those mountains have higher altitudes and smaller amount of annual precipitation compared with the adjacent basins. Less N leaching happened in those regions. Meanwhile, both regions in the tropics that are dominant with TrBEF. Thus, it is possible that N_2O emission was higher in this circumstance. In the Northeastern Brazil and the Southeast coast of Australia, both regions are along the coast. Both regions were not xeric according to the annual precipitation data used in this study. In the Northeastern Brazil, the dominant vegetation type is still TrBEF. Similarly, less N leaching and proper soil water content might cause higher amount of N_2O emissions. In the east coast of Australia, anthropogenic activities contributed a large amount of N deposition in 1860 compared to other regions of Australia. Several grids with higher emissions were dominant with Temperate Broadleaf Evergreen Forest (TBEF). Meanwhile, the precipitation was generally higher along the Australian coast. Thus, higher N deposition with proper precipitation might cause this high N_2O emission.

Technical Points

1. Line 41: This statement ignores that some anthropogenic emissions were already present prior to or at the beginning of the industrial revolution.

Response:

It is true that there existed anthropogenic N_2O emission before 1860; however, the total amount is substantially lower than the contemporary human-induced N_2O emissions. The description of anthropogenic emissions in the pre-industrial era was added, shown as "Human-induced biogenic N_2O emissions are calculated by subtracting the pre-industrial emissions (Tian et al., 2016), even though a small amount of anthropogenic N_2O emissions was present before 1860, which was estimated as 1.1 Tg N yr^{-1} in 1850 by Syakila and Kroeze (2011) and 0.7 (0.6–0.8) Tg N yr^{-1} in 1860 by Davidson (2009)."

2. Line 55: Add recent results from Prather et al. 2015.

Response:

The latest study done by Prather et al. (2015) has been added into line 56, shown as "Prather et al. (2015) provided an estimate of the pre-industrial emissions (total natural emission: 10.5 Tg N yr^{-1}) based on the then-most-recent model study with a corrected lifetime of 116±9 years."

3. Line 70: Change "is" to "are" because the word "data" is plural: "the data are".

Response:

It has been revised.

4. Line 178: Use estimate from Prather et al. 2015.

Response:

We have removed the section 2.4.2 and section 3.2, which described the one-box model validation of simulation results. Thus, there is no need to replace the N_2O lifetime in this section. In addition, we added the comparison of the estimate in this study with the estimation by Prather et al. (2012, 2015) in the section 3.2.

5. Line 312: Consider other estimates, such as those of Voss et al. 2013.

Response:

We carefully read the paper from Voss et al. (2013) and found that their estimates were directly from the IPCC AR4 (Table 7.7 in Chapter 7). In their paper, the N_2O emission from ocean was 5.5 Tg N yr^{-1} because they considered the emissions (1.7 Tg N yr^{-1}) from "rivers, estuaries, and coastal zones" as the marine emissions. Thus, the average marine emissions are 3.8 Tg N yr^{-1}, as shown in Table 6.9 of Chapter 6 in the IPCC AR5.

6. Figure 2. I don't understand the units. How can these units of crop area apply to each individual pixel?

Response:

To avoid the confusion of the unit, it has been changed from "km^2" to "km^2/grid". The size of individual pixel is 0.5 degree, equivalent to around 2500 km^2 at the equator. Meanwhile, we have crop area fraction in each pixel (mentioned in the section 2.1 & 2.2). Then, in each grid, crop area fraction multiplying the pixel size represents the crop area. The numbers in the legend mean the cropland area in each 0.5-degree pixel.

7. Figure 3. The data used for this graph should be referenced.

Response:

All papers that used for the graph cited in the new version.

8. Figure 5. The bottom panel is all that is needed. The top panel is redundant. However, you could also add a panel of mean flux per hectare, which would be useful, because it is difficult to compare fluxes across continents when the contents have such different total areas.

Response:

We agree with the reviewer. We have removed the top panel. Instead, we added a panel of N_2O emission rates per unit area (g N m^{-2} yr^{-1}) with uncertainty ranges at continental-level in 1860, as shown in Fig. 5 (a).

9. Figure 6. The two panels are largely redundant. The pie chart could include both the percentage of the total and the estimate of Tg/yr, which would obviate the need for the upper panel. However, again, the mean flux per hectare by biome would be an interesting panel to add.

Response:

We agree with the reviewer. We have removed the top panel. Instead, we added a panel of N_2O emission rates per unit area (g N m^{-2} yr^{-1}) with uncertainty ranges at biome-scale in 1860, as shown in Fig. 6 (a). In addition, we added the biome-scale emission amounts and their uncertainty ranges into the pie chart, as shown in Fig. 6 (b).

10. Table 2. The number of significant figures shown is excessive. I suggest rounding to the nearest Gg. The uncertainties are such that any fraction of a Gg is meaningless.

Response:

Since the one-box model section has been removed, Table 1 was deleted, and "Table 2" was changed to "Table 1". The uncertainties have been removed. We added the biome- and continental-scale N_2O emissions in the supplementary material (Table S2). For the mean annual N_2O emissions (Tg N yr^{-1}) and emission rate per unit area (kg N ha^{-1} yr^{-1}), we have listed all numbers in the Table S3. We included the revised figures as below:

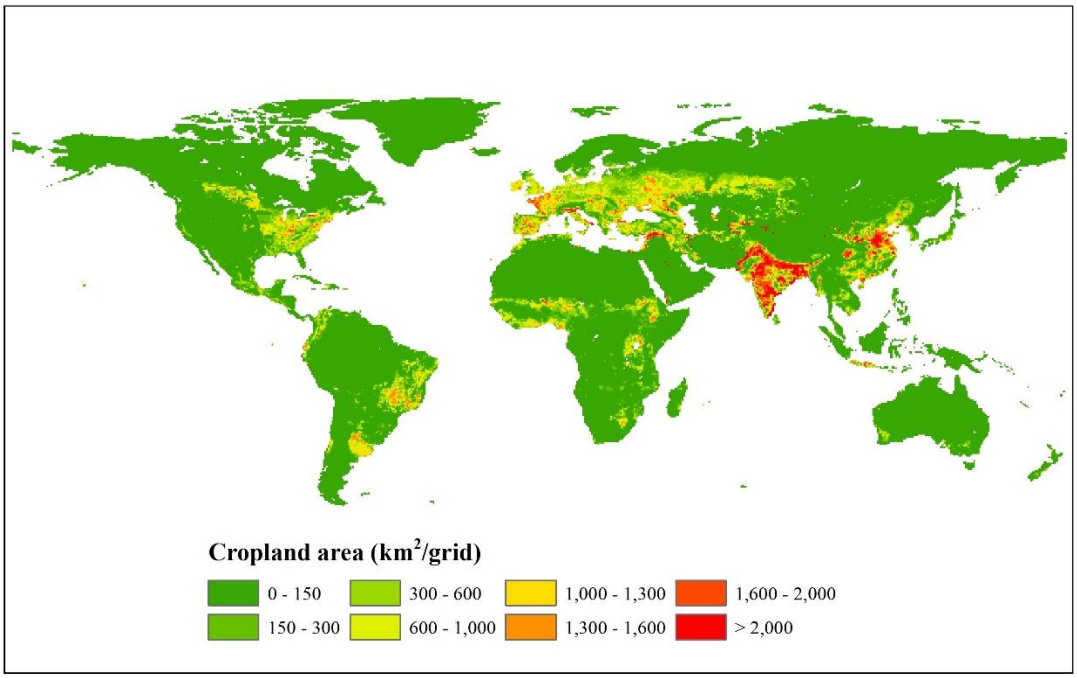

Fig. 2 The spatial distribution of cropland area in 1860.

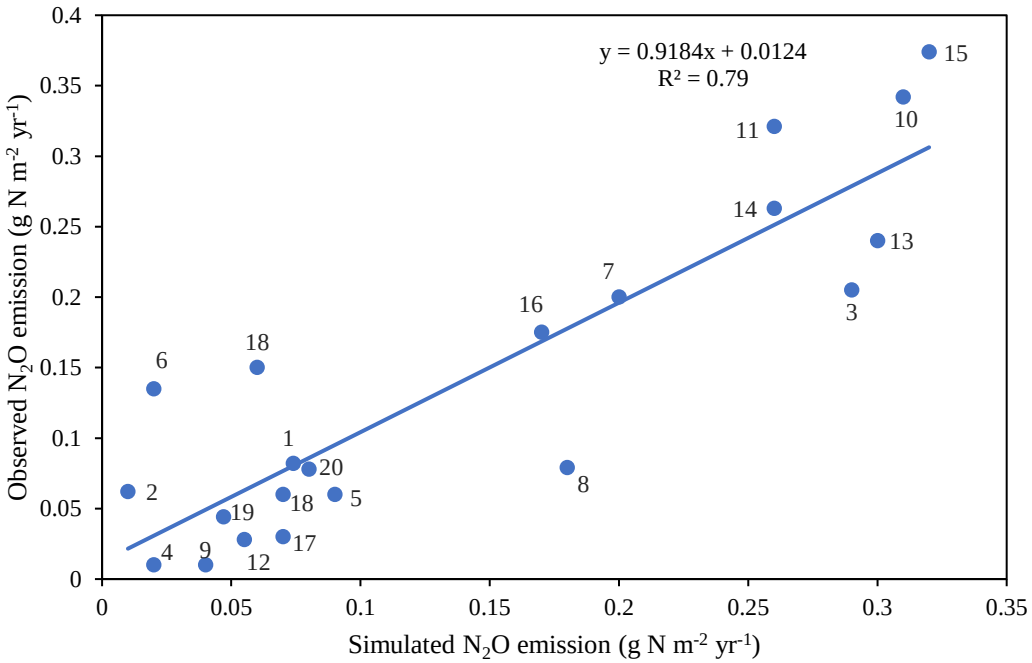

Fig. 3 The comparison of the DLEM-simulated N_2O emissions with field observations. All sites were described in the supplementary material (Table S1).

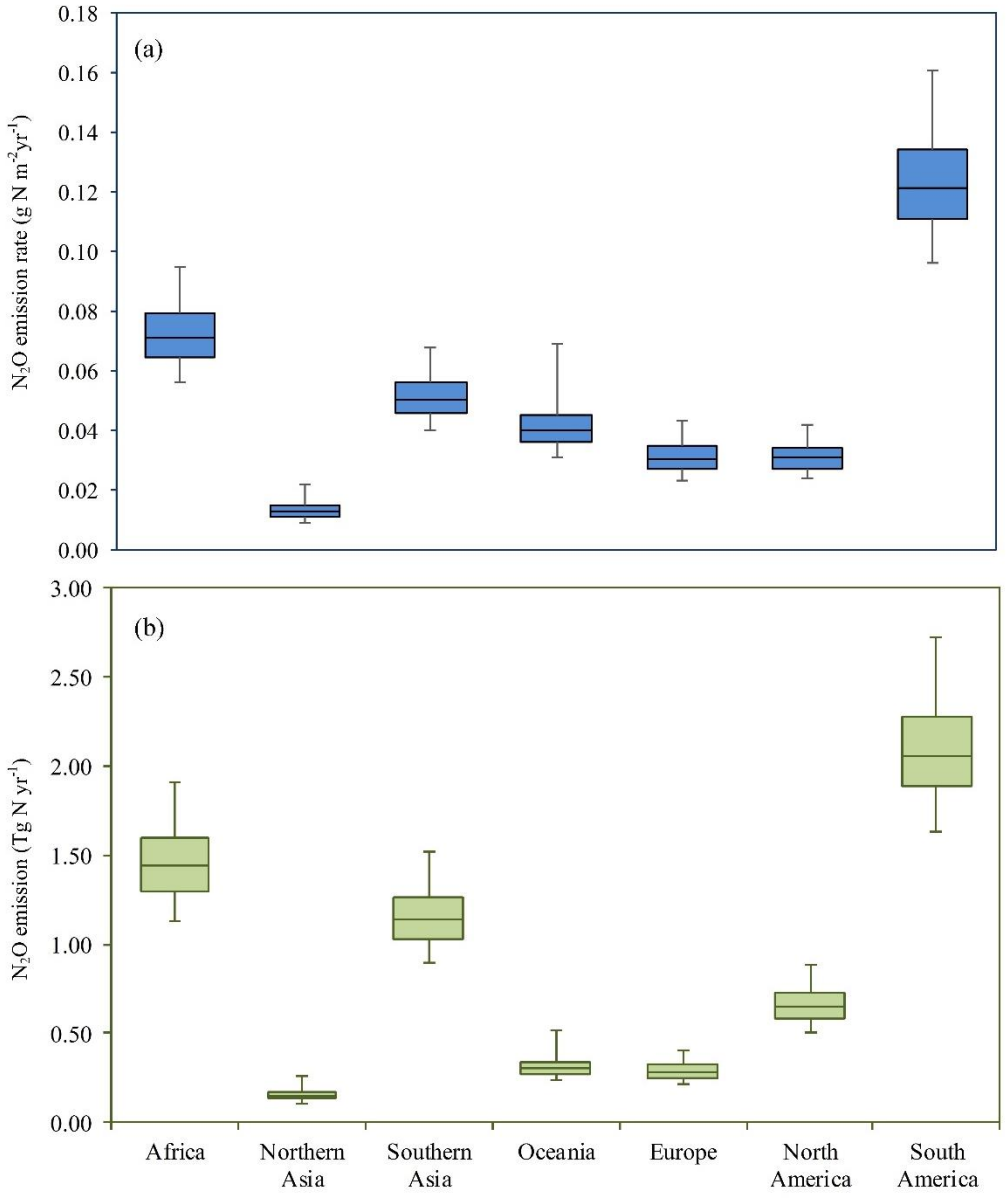

Fig. 5 Estimated N_2O emission rates (a) and emissions (b) with uncertainty ranges at continental-level in 1860. Solid line within each box refers to the median value of N_2O emission rate or amount.

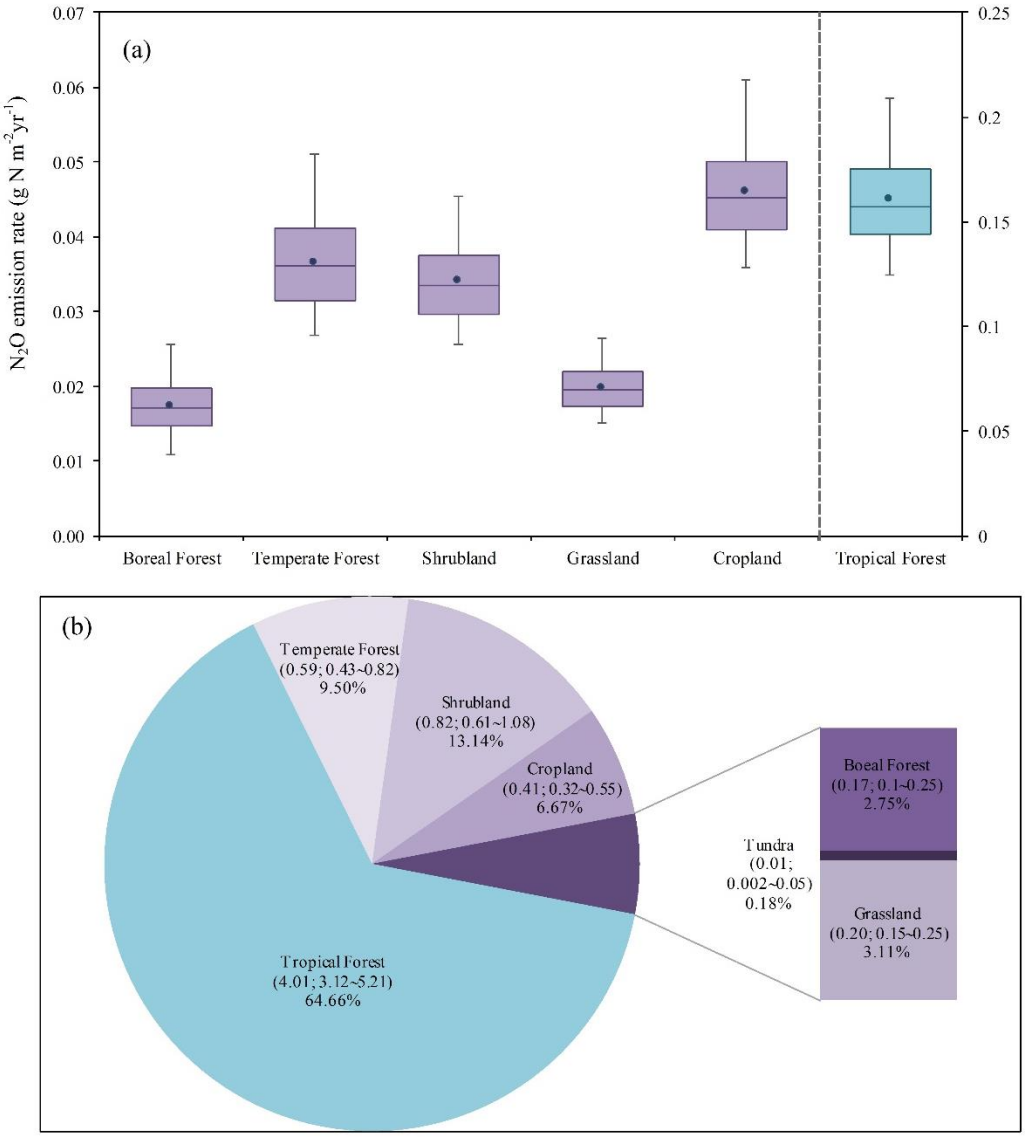

Fig. 6 (a) Estimated N_2O emission rate at biome-level in 1860 with the median value (solid line), the mean (solid dot), and the uncertainty range of emission rates from different biomes. The emission rate in the tundra was removed because of the extremely small value (less than 0.003g N m^{-2} yr^{-1}); (b) Estimated N_2O emission (Tg N yr^{-1}) with uncertainty ranges and its percentage (%) at biome-level in 1860.

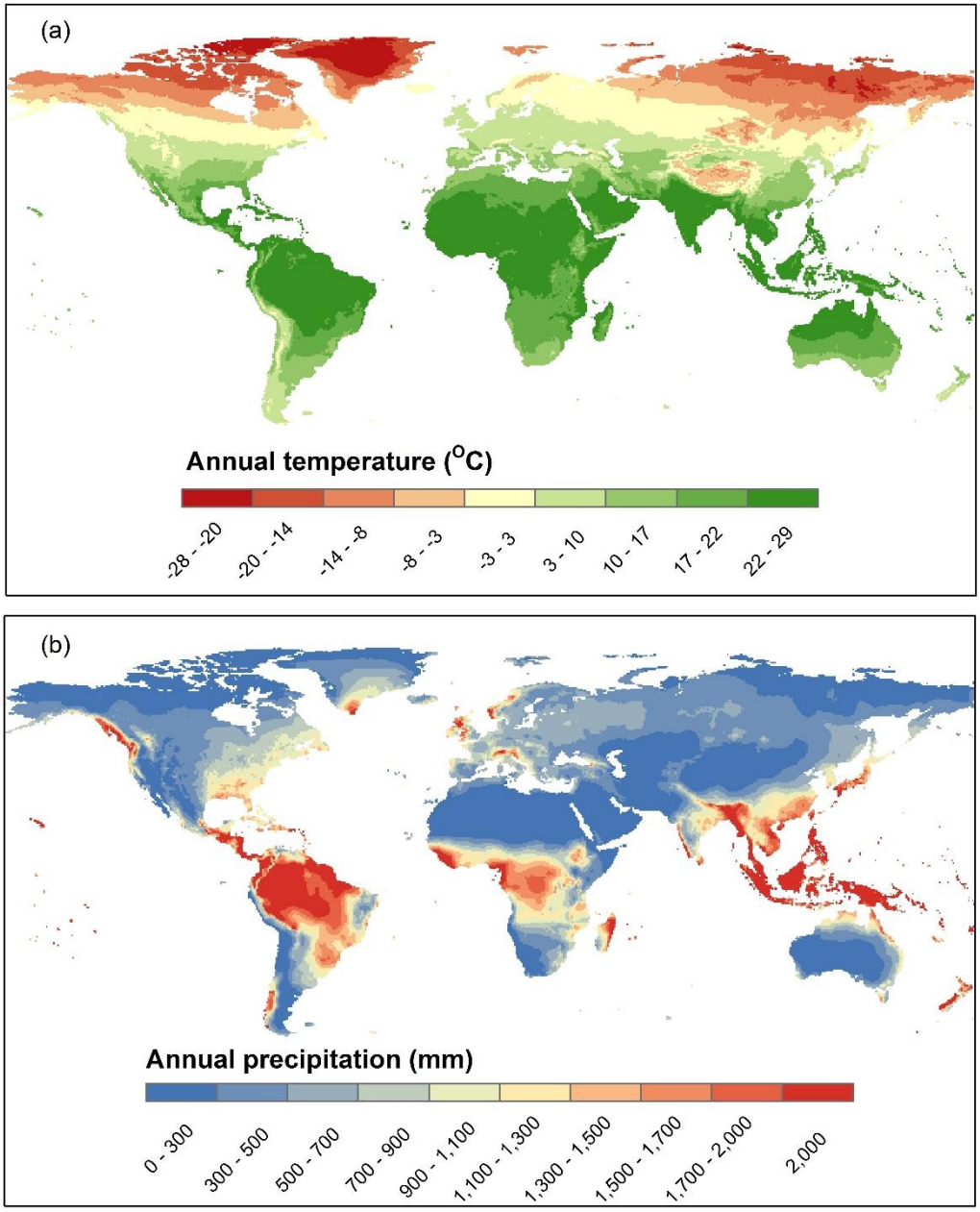

Figure S2. (a) The average annual temperature during 1901–1930; (b) The average annual precipitation during 1901–1930.

Table S1. The description of field measurements from natural vegetation in different sites.

Number	PFT	location		Year	References
		Longitude	Latitude		
1	Forest: Spruce	11°25'E	48°46'N	1993-1995	Butterbach-Bahl et al., 1998
2	Forest: Spruce	09°34'E	51°46'N	2007-2008	Eickenscheidt and Brumme, 2012
3	Forest: Liana canopy	55°31'W	3°59'S	1998-2000	Davidson et al., 2004
4	Forest: Douglas-fir	124°30'W	44°00'N	2007-2008	Erickson and Perakis, 2014
5	Grassland	09°42'E	51°46'N	2008-2009	Hoeft et al., 2012
6	Forest	156°14'W	20°48'N	2000-2001	Holtgrieve et al., 2006
7	Forest: Spruce &Oak	19°57'–58'E	47°53'N	2002-2003	Horváth et al., 2006
8	Forest: Beech	16°15'E	48°14'N	2002-2004	Kitzler et al., 2006
9	Grassland	104°42'W	40°50'N	1997-2000	Mosier et al., 2002
10	Tropical rain forest	145°30'E	17°30'S	1997-1999	Breuer et al., 2000
11	Tropical rain forest	63°00'W	10°00'S	–	Stehfest and Bouwman, 2006
12	Savanna	28°30'E	24°30'S	1994	Scholes et al., 1997
13	Tropical forest	47°30'W	3°00'S	1987	Luizão et al., 1989
14	Tropical forest	115°30'E	2°00'S	1998-1999	Hadi et al., 2000
15	Tropical forest	84°00'W	10°26'N	1990-1991	Keller and Reiners, 1994
16	Subtropical forest	66°00'W	18°00'N	1995-1996	Erickson et al. 2001
17	Temperate forest	116°30'E	39°30'N	1997-1998	Sun and Xu, 2001
18	Temperate forest	89°00'W	43°00'N	1979-1981	Goodroad and Keeney, 1984
19	Grassland	116°04'E	43°26'N	1995	Chen et al., 2000
20	Temperate forest	126°55'E	41°23'N	1994-1995	

Table S3 The estimated mean N_2O emissions and emission rates per unit area at continental- and biome-scale with the uncertainty ranges. kg N ha^{-1} yr^{-1} = 0.1 g N m^{-2} yr^{-1}

Continental-scale	Europe	North America	South America	Southern Asia	Northern Asia	Oceania	Africa
N_2O emissions (Tg N yr^{-1})	0.29 (0.21~0.40)	0.66 (0.51~0.89)	2.09 (1.63~2.73)	1.16 (0.90~1.52)	0.16 (0.11~0.26)	0.31 (0.23~0.52)	1.46 (1.13~1.91)
N_2O emission rate (kg N ha^{-1})	0.31 (0.23~0.43)	0.31 (0.24~0.42)	1.23 (0.96~1.61)	0.52 (0.40~0.68)	0.13 (0.09~0.22)	0.41 (0.31~0.69)	0.73 (0.56~0.95)
Biome-scale	Boreal Forest	Tropical Forest	Temperate Forest	Shrubland	Grassland	Cropland	Tundra
N_2O emissions (Tg N yr^{-1})	0.17 (0.10~0.25)	4.01 (3.12~5.21)	0.59 (0.43~0.82)	0.82 (0.61~1.08)	0.20 (0.15~0.25)	0.41 (0.32~0.55)	0.01 (0.002~0.05)
N_2O emission rate (kg N ha^{-1})	0.17 (0.11~0.26)	1.60 (1.25~2.09)	0.37 (0.27~0.51)	0.34 (0.26~0.45)	0.2 (0.15~0.26)	0.46 (0.36~0.61)	–

References:

Chapuis-Lardy, L., Wrage, N., Metay, A., CHOTTE, J. L., and Bernoux, M.: Soils, a sink for N_2O? A review, Global Change Biology, 13, 1-17, 2007.

Ciais, P., Sabine, C., Bala, G., Bopp, L., Brovkin, V., Canadell, J., Chhabra, A., DeFries, R., Galloway, J., Heimann, M. and Jones, C.: Carbon and other biogeochemical cycles. In Climate Change 2013: The Physical Science Basis. Contribution of Working Group I to the Fifth Assessment Report of the Intergovernmental Panel on Climate Change. Cambridge University Press, 465-570, 2014.

Davidson, E. A., Keller, M., Erickson, H. E., Verchot, L. V., and Veldkamp, E.: Testing a Conceptual Model of Soil Emissions of Nitrous and Nitric Oxides: Using two functions based on soil nitrogen availability and soil water content, the hole-in-the-pipe model characterizes a large fraction of the observed variation of nitric oxide and nitrous oxide emissions from soils, Bioscience, 50, 667-680, 2000.

Davidson, E. A.: The contribution of manure and fertilizer nitrogen to atmospheric nitrous oxide since 1860, Nature Geoscience, 2, 659-662, 2009.

Davidson, E. A., and Kanter, D.: Inventories and scenarios of nitrous oxide emissions, Environmental Research Letters, 9, 105012, 2014.

Denman K., Brasseur G., Chidthaisong A., Ciais P. M., Cox P., Dickinson R., Hauglustaine D., Heinze C., Holland E., Jacob D., Lohmann U., Ramachandran S., da Silva Dias P., Wofsy S. and Zhang X.: Couplings Between Changes in the Climate System and Biogeochemistry. In: Climate Change 2007: The Physical Science Basis. Contribution of Working Group I to the Fourth Assessment Report of the Intergovernmental Panel on Climate Change [Solomon S., Qin D., Manning M., Chen Z., Marquis M., Averyt K. B., Tignor M., and Miller H. (eds.)]. Cambridge University Press, Cambridge, United Kingdom and New York, NY, USA, 501-566, 2007.

Mertz, O., Müller, D., Sikor, T., Hett, C., Heinimann, A., Castella, J.-C., Lestrelin, G., Ryan, C. M., Reay, D. S., Schmidt-Vogt, D., Danielsen, F., Theilade, I., Noordwijk, M. v., Verchot, L. V., Burgess, N. D., Berry, N. J., Pham, T. T., Messerli, P., Xu, J., Fensholt, R., Hostert, P., Pflugmacher, D., Bruun, T. B., Neergaard, A. d., Dons, K., Dewi, S., Rutishauser, E., Sun, and Zhanli: The forgotten D: challenges of addressing forest degradation in complex mosaic landscapes under REDD+, Geografisk Tidsskrift-Danish Journal of Geography, 112, 63-76, 10.1080/00167223.2012.709678, 2012.

Mitchell, T. D., and Jones, P. D.: An improved method of constructing a database of monthly climate observations and associated high-resolution grids, International journal of climatology, 25, 693-712, 2005.

New, M., Hulme, M., and Jones, P.: Representing twentieth-century space–time climate variability. Part I: Development of a 1961–90 mean monthly terrestrial climatology, Journal of climate, 12, 829-856, 1999.

Prather, M. J., Holmes, C. D., and Hsu, J.: Reactive greenhouse gas scenarios: Systematic exploration of uncertainties and the role of atmospheric chemistry, Geophysical Research Letters, 39, 2012.

Prather, M. J., Hsu, J., DeLuca, N. M., Jackman, C. H., Oman, L. D., Douglass, A. R., Fleming, E. L., Strahan, S. E., Steenrod, S. D., and Søvde, O. A.: Measuring and modeling the lifetime of nitrous oxide including its variability, Journal of Geophysical Research: Atmospheres, 120, 5693-5705, 2015.

Stehfest, E., and Bouwman, L.: N_2O and NO emission from agricultural fields and soils under natural vegetation: summarizing available measurement data and modeling of global annual emissions, Nutrient Cycling in Agroecosystems, 74, 207-228, 2006.

Syakila, A., and Kroeze, C.: The global nitrous oxide budget revisited, Greenhouse Gas Measurement and Management, 1, 17-26, 2011.

Kim D. G., Thomas, A. D., Pelster D., Rosenstock, T. S., Sanz-Cobena A.: Greenhouse gas emissions from natural ecosystems and agricultural lands in sub-Saharan Africa: synthesis of available data and suggestions for further research, Biogeosciences, 13, 4789, 2016.

Tian, H., Lu, C., Ciais, P., Michalak, A. M., Canadell, J. G., Saikawa, E., Huntzinger, D. N., Gurney, K. R., Sitch, S., and Zhang, B.: The terrestrial biosphere as a net source of greenhouse gases to the atmosphere, Nature, 531, 225-228, 2016.

van Lent, J., Hergoualc'h, K., and Verchot, L.: Reviews and syntheses: Soil N_2O and NO emissions from land use and land use change in the tropics and subtropics: a meta-analysis, Biogeosciences, 12, 2015.

Voss, M., Bange, H. W., Dippner, J. W., Middelburg, J. J., Montoya, J. P., and Ward, B.: The marine nitrogen cycle: recent discoveries, uncertainties and the potential relevance of climate change, Philosophical Transactions of the Royal Society B: Biological Sciences, 368, 20130121, 2013.

Zhuang, Q., Lu, Y., and Chen, M.: An inventory of global N_2O emissions from the soils of natural terrestrial ecosystems, Atmospheric Environment, 47, 66-75, 2012.

Dear reviewer #2,

Many thanks for your highly valuable comments! All your questions have been answered as follows:

1. The country-level analysis does not make much sense as a large amount of countries had different boundaries compared to present. In line 396, those country-level emissions might need to be removed.

Response:

Yes, the current country boundaries are different from that in the preindustrial era. Here we just want to look at the regional differences in N_2O emission for current country-level from geographical perspective. The region division based on country scale could be more interesting, so we still hope to keep this country-level analysis here.

2. I am little curious to see the small uncertainties in continent-level N_2O show in Figure 5 as the LHS was used and the large uncertainties were shown in below panel in Figure 5.

Response:

The small uncertainty range shown in the upper panel of Fig. 5 was the 95% confidence interval of the mean estimate, as explained in the manuscript. The uncertainty range of pre-industrial N_2O emissions was present using the minimum and maximum estimate (4.76–8.13 Tg N yr^{-1}) in this study, which was consistent with other studies, such as the reported estimates in the IPCC AR5. Here, the Bootstrap resampling method was used to define the uncertainty bounds of global mean N_2O emission (6.20 Tg N yr^{-1}) (shown in line 216-219 of previous manuscript). It was used to verify the stability of the LHS approach. The 95% confidence intervals (6.03-6.36 Tg N yr^{-1}) of the mean did not represent the uncertainty range for pre-industrial N_2O emission in this study. In order to avoid the confusion, we will not report this narrow range in the revised manuscript.

Meanwhile, the first reviewer also suggested to remove it because the upper and below panel deliver the same information. Instead, we replaced the Fig. 5(a) with a panel of N_2O emission rates per unit area (g N m^{-2} yr^{-1}) with uncertainties.

3. The model implementation is not clear. I assume this study is based on a steady state or semi-steady state simulation. The equilibrium run was for 1860, followed by a spinup. The transient run

was driven with climate data in 1860 (line 153). What is the data source? If the equilibrium run was based on 1860 data (most). Then, there are small discrepancies among spinup and transient runs. A comparison between equilibrium and transient run might be needed. If there are no big differences, using equilibrium run might be more convincing, as most driving forces were 1860 except climate data of 1901-1930. If the authors really want to have a transient run, the model simulations should start even further to capture the legacy impacts of natural and anthropogenic impacts, particularly the land use change.

Response:

Yes, this study was based on steady state simulation. The data sources for equilibrium run were all based on the data in 1860. Our transient run for 1860 was actually an extension of the equilibrium run. We don't have transient data before 1860 to realistically include the legacy effects from land use change, climate, etc. before 1860. The reason we ran this transient run was to avoid the abnormal fluctuations after equilibrium run, rather than capturing the legacy impacts. Fig. 4 in the manuscript is the result from equilibrium run. We made a comparison between the equilibrium and transient results for 1860 (Fig. S3). Although there were small differences for some grid cells between the two simulation results, the simulation results for the equilibrium run were similar to the transient run as a whole.

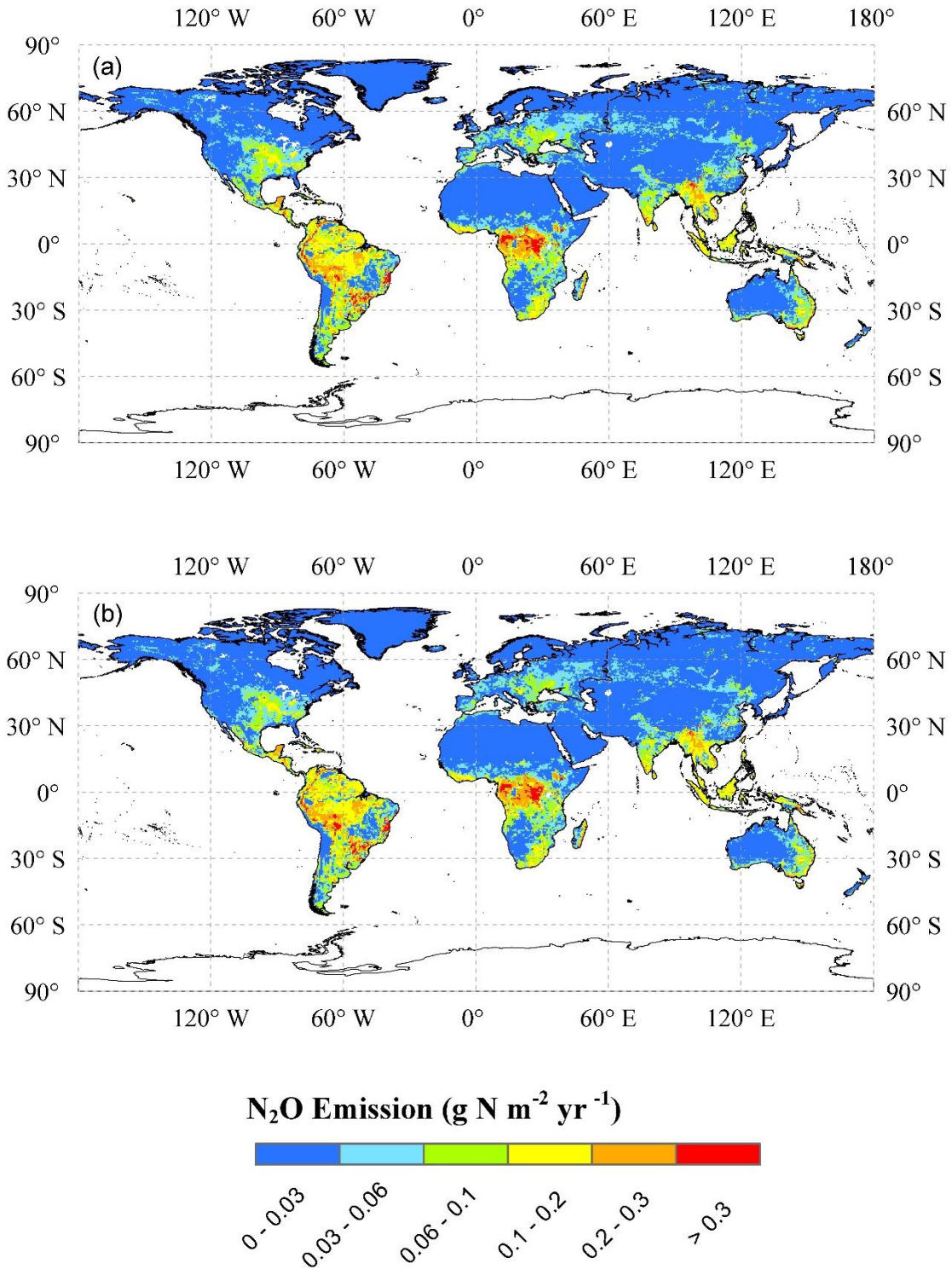

Fig. S3 (a) The spatial distribution of global N_2O emission from the equilibrium run; (b) The spatial pattern distribution of global N_2O emission from the transient run.

All changes were marked as blue in the revised manuscript.

A list of relevant changes:

1. In the **introduction** section, we added the recent results by Prather et al. (2015) (Line 55-57). Meanwhile, we included the estimation of human-induced N_2O emissions in 1860 from previous studies (Line 37-41). In addition, we addressed the objectives of this study at the end of the introduction section (Line 72-77).

2. In the **methodology** section, as suggested by the reviewer, we have removed the one-box model approach.

3. In the **result and discussion** section, as suggested by the reviewer, we removed the results from the one-box approach, while we added the comparison of our study with the previous estimations based on the top-down methodology (Section 3.2). Moreover, we added one section to discuss the N_2O budget in the pre-industrial era (Section 3.4).

4. In the **future research needs** section, we also made some changes, which were marked as blue (Line 353-356).

5. In the **references**, we added all missing references and marked as blue.

For tables and figure:

1. As suggested by the reviewer, we have added the site number in Table S1 and Fig. 3.

2. As suggested by the reviewers, we have revised the top panels of Fig. 5 and Fig. 6, respectively.

3. In Table 1, we have removed the uncertainty ranges for N_2O emissions in each country.

4. We added Table S3 in the supplementary material, which shows the pre-industrial N_2O emission amounts and rates at the continental- and biome-scale with the uncertainty ranges.

Estimation of pre-industrial nitrous oxide emissions from the land biosphere

Rongting Xu[1], Hanqin Tian[1,2], Chaoqun Lu[3], Shufen Pan[1,2], Jian Chen[4,1], Jia Yang[1], Bowen Zhang[1]

[1] International Center for Climate and Global Change Research and School of Forestry and Wildlife Sciences, Auburn University, Auburn, AL 36849, USA

[2]State Key Laboratory of Urban and Regional Ecology, Research Center for Eco-Environmental Sciences, Chinese Academy of Sciences, Beijing 100085, China

[3]Department of Ecology, Evolution, & Organismal Biology, Iowa State University, Ames, IA 50011, USA

[4] College of Sciences and Mathematics, Auburn University, Auburn, AL 36849, USA

Correspondence to: Hanqin Tian (tianhan@auburn.edu)

Abstract. To accurately assess how increased global nitrous oxide (N_2O) emission has affected the climate system requires a robust estimation of the pre-industrial N_2O emissions since only the difference between current and pre-industrial emissions represents net drivers of anthropogenic climate change. However, large uncertainty exists in previous estimates of pre-industrial N_2O emissions from the land biosphere, while pre-industrial N_2O emissions at the finer scales such as regional, biome, or sector have not yet well quantified. In this study, we applied a process-based Dynamic Land Ecosystem Model (DLEM) to estimate the magnitude and spatial patterns of pre-industrial N_2O fluxes at the biome-, continental-, and global-level as driven by multiple environmental factors. Uncertainties associated with key parameters were also evaluated. Our study indicates that the mean of the pre-industrial N_2O emission was approximately 6.20 Tg N yr^{-1}, with an uncertainty range of 4.76 to 8.13 Tg N yr^{-1}. The estimated N_2O emission varied significantly at spatial- and biome-levels. South America, Africa, and Southern Asia accounted for 34.12%, 23.85%, 18.93%, respectively, together contributing of 76.90% of global total emission. The tropics were identified as the major source of N_2O released into the atmosphere, accounting for 64.66% of the total emission. Our multi-scale estimates provide a robust reference for assessing the climate forcing of anthropogenic N_2O emission from the land biosphere

1 Introduction

Nitrous oxide (N_2O) acts as the third-most important greenhouse gas (GHG) after carbon dioxide (CO_2) and methane (CH_4), largely contributing to the current radiative forcing (Myhre et al., 2013). Nitrous oxide is also the most long-lived reactant, resulting in the destruction of stratospheric ozone (Prather et al., 2015; Ravishankara et al., 2009). The atmospheric concentration of N_2O increased from 275 to 329 parts per billion (ppb) since the pre-industrial era until 2015 at a rate of approximately 0.26% per year, as a result of human activities (Davidson, 2009; Forster et al., 2007; NOAA2006A). The human-induced N_2O emissions from the terrestrial biosphere have offset about half of terrestrial CO_2 sink and contributed a net warming effect on the climate system (Tian et al., 2016). In the contemporary period, anthropogenic N_2O emissions are mainly caused by the expansion in agricultural land area and increase in nitrogen (N) fertilizer application, as well as industrial activities, biomass burning and indirect emissions from reactive N (Galloway et al., 2004; Reay et al., 2012). Human-induced biogenic N_2O emissions were calculated by subtracting the pre-industrial emissions (Tian et al., 2016), even though a small amount of anthropogenic N_2O emissions was present before 1860, which was estimated as 1.1 Tg N yr^{-1} in 1850 by Syakila and Kroeze (2011) and 0.7 (0.6–0.8) Tg N yr^{-1} (including anthropogenic biogenic emissions from soils and biomass burning) in 1860 by Davidson (2009). Therefore, it is necessary to provide a robust reference of pre-industrial N_2O emission for assessing the climate forcing of anthropogenic N_2O emission from the land biosphere.

Numerous studies have reported the sources and estimates of N_2O emission since the pre-industrial era (Davidson and Kanter, 2014; Galloway et al., 2004; Kroeze et al., 1999; Prather et al., 2012, 2015; Syakila and Kroeze, 2011). According to the Intergovernmental Panel on Climate Change Guidelines (IPCC, 1997), the global N_2O emission evaluated by Kroeze et al. (1999) is 11 (8–13) Tg N yr^{-1} (Natural soils: 5.6–6.6 Tg N yr^{-1}, Anthropogenic: 1.4 Tg N yr^{-1}), which is consistent with the estimation from global pre-agricultural

N_2O emissions in soils (6–7 Tg N yr^{-1}) (Bouwman et al., 1993). While taking into account the new emission factor from the IPCC 2006 Guidelines (Denman et al., 2007), Syakila and Kroeze (2011) conducted an updated estimate based on the study of Kroeze et al. (1999) and reported that the global pre-industrial N_2O emission is 11.6 Tg N yr^{-1} (Anthropogenic: 1.1 Tg N yr^{-1}, Natural soils: 7 Tg N yr^{-1}). Based on the IPCC AR5, Davidson and Kanter (2014) indicated that the central estimates of both top-down and bottom-up approaches for pre-industrial natural emissions were in agreement at 11 (10–12) Tg N yr^{-1}, including natural emission from soils at 6.6 (3.3–9.0) Tg N yr^{-1} (Syakila and Kroeze, 2011). Prather et al. (2015) provided an estimate of the pre-industrial emissions (total natural emission: 10.5 Tg N yr^{-1}) based on the most recent study with a corrected lifetime of 116±9 years. Although these previous estimates intent to provide a baseline of pre-industrial N_2O emission at global-level, information on pre-industrial N_2O emissions on fine resolutions such as biome-, sector- or country-, and regional-levels remains unknown but needed for effective greenhouse gas accounting and climate policy-making.

Large uncertainties in the estimates of pre-industrial N_2O emission could derive from different approaches (i.e. top-down and bottom-up), as mentioned above. Nitrous oxide, as an important component of the N cycle, is produced by biological processes such as denitrification and nitrification in terrestrial and aquatic systems (Schmidt et al., 2004; Smith and Arah, 1990; Wrage et al., 2001). In order to accurately estimate pre-industrial N_2O emissions using the process-based Dynamic Land Ecosystem Model (DLEM, Tian et al., 2010), uncertainties associated with key parameters, such as maximum nitrification and denitrification rates, biological N fixation (BNF) rates, and the adsorption coefficient for soil ammonium (NH_4^+) and nitrate (NO_3^-), were required to be considered in model simulation. Upper and lower limits of these parameters were used to derive a range of pre-industrial N_2O emissions from terrestrial ecosystems.

In this study, the DLEM was used to simulate global N_2O emission in the pre-industrial era at a resolution of 0.5° × 0.5° latitude/longitude. Since there are no observational data of N_2O emission in the

pre-industrial period, the estimates of natural emission from Prather et al. (2012, 2015) were used to validate the simulation results. In addition, site-level N_2O emissions from different natural vegetation were used to test model performance in the contemporary period. The objectives in this study include: (1) providing a global estimation of N_2O emission from terrestrial soils in 1860, (2) offering the continental-, biome-, and country-scale N_2O emission amounts and flux rates, and (3) discussing uncertainties in estimating N_2O budget in the pre-industrial era. Finally, our estimates at global- and biome-scales were compared with previous estimates.

2 Methodology

2.1 Model description

The DLEM is a highly integrated process-based ecosystem model, which combines biophysical characteristics, plant physiological processes, biogeochemical cycles, vegetation dynamics and land use to make daily, spatially-explicit estimates of carbon, nitrogen and water fluxes and pool sizes in terrestrial ecosystems from site- and regional- to global-scales (Lu and Tian, 2013; Tian et al., 2012; Tian et al., 2015). The DLEM is characterized of cohort structure, multiple soil layer processes, coupled carbon, water and nitrogen cycles, multiple GHG emissions simulation, enhanced land surface processes, and dynamic linkages between terrestrial and riverine ecosystems (Liu et al., 2013; Tian et al., 2010, 2015). The previous results of GHG emissions from DLEM simulations have been validated against field observations and measurements at various sites (Lu and Tian, 2013; Ren et al., 2011; Tian et al., 2010, 2011; Xu et al. 2012; Zhang et al., 2016). The estimates of water, carbon, and nutrients fluxes and storages were also compared with the estimates from different approaches at regional-, continental-, and global-scales (Pan et al., 2014; Tian et al., 2015; Yang et al., 2015). Different soil organic pools and calculations of decomposition rates were described in Tian et al. (2015). The decomposition and nitrogen mineralization processes in the DLEM were described in other publications (Lu and Tian, 2013; Yang et al., 2015).

The N_2O module

Previous work provided a detailed description of trace gas modules in the DLEM (Tian et al., 2010). However, both denitrification and nitrification processes have been modified based on the first-order kinetics (Chatskikh et al., 2005; Heinen, 2006).

In the DLEM, the N_2O production and fluxes are determined by soil inorganic N content (NH_4^+ and NO_3^-) and environmental factors, such as soil texture, temperature, and moisture:

$$F_{N2O} = (R_{nit} + R_{den})F(T_{soil})(1 - F(Q_{wfp})) \quad (1)$$

where F_{N2O} is the N_2O flux from soils to the atmosphere (g N m^2 d^{-1}), R_{nit} is the daily nitrification rate (g N m^2 d^{-1}), R_{den} is the daily denitrification rate (g N m^2 d^{-1}), $F(T_{soil})$ is the function of daily soil temperature on nitrification process (unitless), and $F(Q_{wfp})$ is the function of water-filled porosity (unitless).

Nitrification, a process converting NH_4^+ into NO_3^-, is simulated as a function of soil temperature, moisture, and soil NH_4^+ concentration:

$$R_{nit} = k_{nit}F(T_{soil})F(\psi)C_{NH_4} \quad (2)$$

where k_{nit} is the daily maximum fraction of NH_4^+ that is converted into NO_3^- or gases (d^{-1}), $F(\psi)$ is the soil moisture effect (unitless), and C_{NH_4} is the soil NH_4^+ content (g N m^{-2}). Unlike Chatskikh *et al* (2005), who set k_{nit} to 0.10 d^{-1}, it varies with different plant function types (PFTs) in the DLEM with a range of 0.04 to 0.15 d^{-1}. The detailed calculations of $F(T_{soil})$ and $F(\psi)$ were described in Pan et al. (2015) and Yang et al. (2015).

Denitrification is the process that converts NO_3^- into three types of gases, namely, nitric oxide, N_2O, dinitrogen. The denitrification rate is simulated as a function of soil temperature, water-filled porosity, and NO_3^- concentration C_{NO_3} (g N g^{-1} soil):

$$R_{den} = \alpha F(T_{soil}) F(Q_{wfp}) F_N(C_{NO_3}) \quad (3)$$

where $F_N(C_{NO_3})$ is the dependency of the denitrification rate on NO_3^- concentration (unitless), and α is the maximum denitrification rate (g N m^{-2} d^{-1}). The detailed calculations of $F(Q_{wfp})$, $F_N(C_{NO_3})$ and α were described in Yang et al. (2015).

In each grid cell, there are four natural vegetation types and one crop type. The sum of N_2O emission in each grid/d^{-1} is calculated by the following formula:

$$E = \sum_{i=1}^{62481} \sum_{j=1}^{5} (N_{ij} \times f_{ij}) \times A_i \times 10^6 / 10^{12}, \ i = 1, \cdots, 62481, j = 1, \cdots, 5 \quad (4)$$

where E is the daily sum of N_2O emission from all plant functional types (PFTs) in total grids (Tg N/yr^{-1} d^{-1}); N_{ij} (g N/m^2) is the N_2O emission in the grid cell i for PFT j; f_{ij} is the fraction of cell used for PFT j in grid cell i; and A_i (km^2) is the area of the ith grid cell. 10^6 is to convert km^2 to m^2 and 10^{12} is to convert g to Tg.

2.2 Input datasets

Input data to drive DLEM simulation include static and transient data (Tian et al., 2010). Several additional data sets were generated to better represent terrestrial environment in the pre-industrial period as described below. The natural vegetation map was developed based on LUH (Hurtt et al., 2011) and SYNMAP (Jung et al., 2006), which rendered the fractions of 47 vegetation types in each 0.5° grid. These 47 vegetation types were converted to 15 PFTs used in the DLEM through a cross-walk table (Fig. 1). Cropland distribution in 1860 were developed by aggregating the 5-arc minute resolution HYDE v3.1 global cropland distribution data (Fig. 2). Half degree daily climate data (including average, maximum, minimum air temperature, precipitation, relative humidity, and shortwave radiation) were derived from CRU-NCEP climate forcing data (Wei et al., 2014). As global climate dataset was not available prior to the year 1900, long-term average climate datasets from 1901 to 1930 were used to represent the initial climate state in

1860. The nitrogen deposition dataset was developed based on the atmospheric chemistry transport model (Dentener, 2006) constrained by the EDGAR-HYDE nitrogen emission data (Aardenne et al., 2001). The nitrogen deposition dataset provided inter-annual variations of NH_x-N and NO_y-N deposition rates. The manure production dataset (1961–2013) was derived from Food and Agriculture organization of the United Nations statistic website ((FAO), http://faostat.fao.org) and defaulted for N excretion rate referred to IPCC Guidelines (Zhang et al., 2017). Estimates of manure production from 1860 to 1960 were retrieved from the global estimates in (Holland et al., 2005).

2.3 Model simulation

The implementation of the DLEM simulation includes three steps: (1) equilibrium run, (2) spin-up run, and (3) transient run. In this study, we first used land use and land cover (LULC) map in 1860, long-term mean climate during 1901–1930, N input datasets in 1860 (the concentration levels of N deposition and manure application rate), and atmospheric CO_2 in 1860 to run the model to an equilibrium state. In each grid, the equilibrium state was assumed to be reached when the inter-annual variations of carbon, nitrogen, and water storage are less than 0.1 g C/m^2, 0.1 g N/m^2 and 0.1 mm, respectively, during two consecutive 50 years. After the model reached equilibrium state, the model was spun up by the detrended climate data from 1901 to 1930 to eliminate system fluctuation caused by the model mode shift from the equilibrium to transient run (i.e., 3 spins with 10-year climate data each time). Finally, the model was run in the transient mode with daily climate data, annual CO_2 concentration, manure application, and N deposition inputs in 1860 to simulate pre-industrial N_2O emissions. Additional description of model initialization and simulation procedure can be found in previous publications (Tian et al., 2010; Tian et al., 2011).

2.4 Model validation

Observations of annual N_2O emission accumulations (g N m^{-2} yr^{-1}) were selected to compare with the simulated emissions in different sites. As there were no field measurements in the pre-industrial era, observations during 1970–2009 were collected to test the model performance in the contemporary period. All environmental factors (climate, CO_2 concentration, soil property, N deposition, LULC) in the exact year were used as input datasets for N_2O simulations. The selected 20 sites over different continents include temperate forest, tropical forest, boreal forest, savanna, and grassland. As shown in Fig. 3, the simulated N_2O emissions have a good correlation with field observations (R^2 = 0.79). It indicates that the DLEM has the capacity to simulate N_2O emissions in the pre-industrial era driven by environmental factors back then. The detailed information at each site can be found in Table S1.

2.5 Estimate of uncertainty

In this study, uncertainties in the simulated N_2O emission were evaluated through a global sensitivity and uncertainty analysis as described in Tian et al. (2011). Based on sensitivity analyses of key parameters that affect terrestrial N_2O fluxes, the most sensitive parameters were identified to conduct uncertainty simulations with the DLEM. These parameters include potential denitrification and nitrification rates, BNF rates, and the adsorption coefficient for soil NH_4^+ and NO_3^- (Gerber et al., 2010; Tian et al., 2015; Yang et al., 2015). The ranges of five parameters were obtained from previous studies. Chatskikh et al. (2005) set k_{nit} as 0.10 d^{-1}; however, it was set in a range of 0.04 to 0.15 d^{-1}, and varied with different PFTs in the DLEM simulations. The uncertainty ranges of potential nitrification rates were based on previous studies (Hansen, 2002; Heinen, 2006); the global pre-industrial N fixation was estimated as 58 Tg N yr^{-1}, ranging from 50–100 Tg N yr^{-1} (Vitousek et al., 2013). The spatial distribution of BNF referred to the estimates by Cleveland et al. (1999). Potential denitrification rate was set in an uncertainty range of 0.025–0.74 d^{-1}, and varied with different PFTs in the DLEM. The uncertainty ranges of the adsorption coefficient were referred to the sensitivity analysis conducted in Yang et al. (2015). Parameters used in the DLEM simulations for

uncertainty analysis were assumed to follow a normal distribution. The Improved Latin Hypercube Sampling (LHS) approach was used to randomly select an ensemble of 100 sets of parameters (R version 3.2.1) (Tian et al., 2011, 2015).

In the DLEM, after the model reached equilibrium state, a spin-up run was implemented using de-trended climate data from 1901 to 1930 for each set of parameter values. Then, each set of the model was run in transient mode in 1860 to produce the result of the pre-industrial N_2O emissions. All results from 100 groups of simulations are shown in the Table S2. The Shapiro–Wilk test was used on 100 sets of results to check the normality of DLEM simulations. It turned out that the distribution is not normal (P value < 0.05, R version 3.2.1), as shown in Fig. S1. Thus, the uncertainty range was represented as the minimum and maximum value of 100 sets of DLEM simulations.

3 Results & discussion

3.1 Magnitude and spatial distribution of the pre-industrial N_2O emission

Our estimation indicates that the global mean soil N_2O emission in the pre-industrial period (1860) was 6.20 Tg N yr^{-1}. We define the parameter-induced uncertainty of our global estimates as a range between the minimum (4.76 Tg N yr^{-1}) and the maximum (8.13 Tg N yr^{-1}) of 100 sets of DLEM simulations. The terrestrial ecosystem in the pre-industrial period acted as a source of N_2O, and its spatial pattern mostly depends on the biome distribution across the global land surface. The spatial distribution of annual N_2O emission in a 0.5° × 0.5° grid (Fig. 4) shows that the strong sources were found near the equator, such as Southeast Asia, Central Africa, and Central America, where N_2O emission reached as high as 0.45 g N m^{-2} yr^{-1}. The weak N_2O sources were observed in the northern areas of North America and Asia, where the estimated N_2O emission was less than 0.001 g N m^{-2} yr^{-1}. The microbial activity in soils determined the rate of nitrification and denitrification processes, which accounts for approximately 70% of global N_2O

emissions (Smith and Arah, 1990; Syakila and Kroeze, 2011). The tropical regions near the equator could provide microbes optimum temperatures and soil moistures to decompose soil organic matter and release more NO_x and CO_2 into the atmosphere (Butterbach-Bahl et al., 2013). Referring to the observational data from field experiments and model simulations in the tropics, it has been supported that the tropics are the main sources of N_2O emissions from natural vegetation (Bouwman et al., 1995; Werner et al., 2007; Zhuang et al., 2012).

In this study, Asia is divided into two parts: Southern Asia and Northern Asia, where the PFTs and climate conditions are significantly contrasting. As shown in Fig. 1, tropical forest and cropland were dominant PFTs in Southern Asia. In contrast, temperate and boreal forests were main PFTs in Northern Asia. The estimates of N_2O emissions from seven land regions are shown in Fig. 5. At continental scale, the N_2O emission was 2.09 (1.63–2.73) Tg N yr^{-1} in South America, 1.46 (1.13–1.91) Tg N yr^{-1} in Africa, and 1.16 (0.90–1.52) Tg N yr^{-1} in Southern Asia. South America, Africa, and Southern Asia accounted for 33.77%, 23.60%, 18.73%, respectively, together which was 76.10% of global total emission. Europe and Northern Asia contributed to 0.45 (0.32–0.66) Tg N yr^{-1}, which was less than 10% of the total emission.

Nitrous oxide emissions varied remarkably among different ecosystems. Forest, grassland, shrub, tundra and cropland contributed 76.90%, 3.11%, 13.14%, 0.18% and 6.67%, respectively, to the total emission globally (Fig. 6). In different biomes, the tropics accounted for more than half of the total N_2O emission, which is comparable to the conclusion made by Bouwman et al. (1993). In the pre-industrial era, the major inputs of reactive N to terrestrial ecosystems were from BNF, which relies on the activity of a phylogenetically diverse list of bacteria, archaea and symbioses (Cleveland et al., 1999; Vitousek et al., 2013). Tropical savannas have been considered as ‘hot spots’ of BNF by legume nodules that provide the major input of available N (Bate and Gunton, 1982). The substantial inputs of N into tropical forests could contribute to higher amount of the gaseous N losses as N_2O or nitrogen gas (Cleveland et al., 2010; Hall

and Matson, 1999). In contrast, as the largest terrestrial biome, boreal forests lack of available N because the rate of BNF is constricted by cold temperatures and low precipitation during growing season (Alexander and Billington, 1986). Morse et al. (2015) conducted field experiments in Northeastern North American forests. They found that denitrification does vary coherently with patterns of N availability in forests, and no significant correlations between atmospheric N deposition, potential net N mineralization and nitrification rates. Thus, it is reasonable that boreal forests contributed to the least amount of N_2O emission among different forests.

As shown in Fig. 2, cropland areas varied spatially. The regions with high cropland area include the entire Europe, India, eastern China, and central-eastern United States. The global N_2O emission from croplands was estimated as 0.41 (0.32–0.55) Tg N yr^{-1}, which is about ten times less than the estimate reported in the IPCC AR5 (Ciais et al., 2014). As no synthetic N fertilizer was applied to the cropland in 1860, leguminous crops were the major source of N_2O emission from croplands, most of which were planted in central-eastern United States (Fig. 4). Rochette et al. (2004) conducted the experiments on the N_2O emission from soybean without application of N fertilizer. Their work was in agreement with the suggestion that legumes may increase N_2O emissions compared with non-BNF crops (Duxbury et al., 1982) The background emission from ground-based experiments was as high as 0.31–0.42 kg N ha^{-1} in Canada (Duxbury et al., 1982; Rochette et al., 2004).

Pre-industrial N_2O emission at country-level could serve as a reference for calculating human-induced N_2O emission in today's nations. We estimated pre-industrial N_2O emissions from seventeen countries that are "hot spots" of N_2O sources in the contemporary period (Table 1). The order of countries was referred to Gerber et al. (2016) that indicated the top seventeen countries in terms of total N application in 2000. Pre-industrial N_2O emissions from natural soils and croplands varied significantly at country-scales. The United States, China, and India were top countries accounted for emissions from pre-industrial croplands.

Countries close to or located in the tropics, such as Mexico, Indonesia, and Brazil, accounted for negligible emissions from croplands, but substantial amount from natural vegetation in the pre-industrial era. Previous studies indicated that agriculture produces the majority of anthropogenic N_2O emissions (Ciais et al., 2014; Davidson and Kanter, 2014). Our estimate at country-scales could be used as a reference to quantify the net increase of N_2O emissions from agriculture activities in countries of "hot spots".

There is a debate that the natural wetlands and peatlands act as sinks or sources of N_2O. Previous studies showed that N_2O emissions from natural peatlands are usually negligible; however, the drained peatlands with lower water tables might act as sources of N_2O (Augustin et al., 1998; Martikainen et al., 1993). High water tables in wetlands might block the activity of nitrifiers and limit the denitrification (Bouwman et al., 1993). The fluxes of N_2O were negligible in the pelagic regions of boreal ponds and lakes due to the limitation of nitrification and/or nitrate inputs (Huttunen et al., 2003). Couwenberg et al. (2011) mentioned that N_2O emissions always decreased after rewetting when conducting field experiments, which had been excluded from their future analysis of GHG emissions in peatlands. Hadi et al. (2005) pointed out that tropical peatlands ranged from sources to sinks of N_2O, highly affected by land-use and hydrological zone. We were incapable to examine N_2O fluxes from wetlands and peatlands in 1860 as human-induced land-use in those ecosystems was unknown. Thus, we excluded the N_2O emissions from wetlands and peatlands in this study.

3.2 Revisit preindustrial global N_2O emission by incorporating top-down estimates

"Top-down" methodology used to estimate N_2O emissions is based on atmospheric measurements and an inversion model (Thompson et al. 2014). Prather et al. (2012) provided an estimate of 9.1±1.0 Tg N yr^{-1} of natural emission in the pre-industrial era using observed pre-industrial abundances of 270 ppb and model estimates of lifetime decreased from 142 years in the pre-industrial era to 131±10 years in the present-day. Later, Prather et al. (2015) re-evaluated N_2O lifetime based on Microwave Limb Sounder satellite

measurements of stratospheric, which was consistent with modeled values in the present-day. The lifetime in the pre-industrial era and present-day was estimated to be 123 and 116±9 years, respectively. The current lifetime increases the pre-industrial natural emission from 9.1±1.0 to 10.5 Tg N yr^{-1}.

Natural sources for N_2O include soil under natural vegetation, oceans, and atmospheric chemistry (Ciais et al., 2014). The emission from atmospheric chemistry was estimated as 0.6 with an uncertainty range of 0.3–1.2 Tg N yr^{-1}. Syakila and Kroeze (2011) estimated global natural emissions from oceans as 3.5 Tg N yr^{-1}. Oceanic emission was estimated as 3.8 with an uncertainty range of 1.8–5.8 Tg N yr^{-1} in the IPCC AR4. However, the uncertainty range became larger (1.8–9.4 Tg N yr^{-1}) in the IPCC AR5. In our study, the simulated N_2O emission was from agricultural and natural soils. The natural emission was estimated as 5.78 (4.4–7.72) Tg N yr^{-1}. Combining the atmospheric chemistry and the ocean emissions in the IPCC AR5 with the natural emissions from our study, the global total natural N_2O emissions were 10.18 (6.5-18.32) Tg N yr^{-1}. The large uncertainty range was attributed to the uncertainty from oceanic emission, atmospheric chemistry emission, and our estimation. The estimated global total amount (10.18 Tg N yr^{-1}) in this study was comparable to the estimate (10.5 Tg N yr^{-1}) by Prather et al. (2015) using the top-down approach.

3.3 Comparison with estimates by bottom-up methodology

"Bottom-up" approach includes the estimations based on inventory, statistical extrapolation of local flux measurements, and process-based modeling (Tian et al., 2016). The global pre-agricultural N_2O emission was estimated as 6.8 Tg N yr^{-1} based on the regression relationship between measured N_2O fluxes and modeled N_2O production indices (Bouwman et al., 1993). This estimate was adopted to retrieve the trends of atmospheric N_2O concentration in Syakila and Kroeze (2011). In our study, the pre-industrial N_2O emission from natural vegetation was estimated as 5.78 (4.4–7.72) Tg N yr^{-1}, which is about 1 Tg N yr^{-1}

lower than the estimate from Bouwman et al. (1993). Estimate from the tropics (± 30° of the equator) was about 4.57 Tg N yr^{-1}, which is 0.83 Tg N yr^{-1} lower than the estimate from Bouwman et al. (1993). For the rest of natural vegetation, our estimate was 1.21 Tg N yr^{-1}, which is close to 1.4 Tg N yr^{-1} estimated in Bouwman et al. (1993).

Although Bouwman et al. (1993) has studied the potential N_2O emission from natural soils, our study provided a first estimate of spatially distributed N_2O emission in 1860 using the biogeochemical process-based model. Bouwman et al. (1993) provided 1° × 1° monthly N_2O emission using the monthly controlling factors without considering the impact of N deposition. In their study, the soil fertility and carbon content were constant for every month, which could not reflect the monthly dynamic changes of carbon and N pools in natural soils. Moreover, although their study has represented a spatial distribution of potential N_2O emission from natural soils, they had not provided the estimate at biome-, continent-, and country-scales. Thus, their result was hardly to be used as a regional reference for the net human-induced N_2O emissions from some "hot spots", such as Southern Asia. In contrast, in our study, using daily climate and N deposition dataset could better reflect the real variation of N_2O emission through the growing season in natural ecosystems. The comparison with field observations during 1997–2001 indicated that the DLEM can catch the daily peak N_2O emissions in Hubbard Brook Forest (Tian et al., 2010) and Inner-Mongolia (Tian et al., 2011).

As far as the N_2O emission from croplands, our estimate is comparable to the estimate of 0.3 (0.29–0.35) Tg N yr^{-1} extracted from Syakila and Kroeze (2011) by digitizing graphs using the Getdata Graph Digitizer. In their study, the estimation was based on the relationship between the crop production and human population during 1500–1970. In contrast, the result in our study was estimated based on the cropland area of specific crop type, mainly soybean, rice, corn, and wheat in 1860.

317 Thus, the DLEM is capable to provide the estimate of N_2O emission from natural ecosystems at
318 regional- and biome-scales with a higher spatial resolution. This could be a useful reference for quantifying
319 effects of human activities such as the LULC change, N fertilizer and manure application, and increasingly
320 atmospheric N deposition on N_2O emissions in different terrestrial ecosystems or sectors in the
321 contemporary period.

322 **3.4 The N_2O budget in the pre-industrial era**

323 The observed N_2O concentration reflects the result of dynamic production and consumption processes in
324 soils as soils act as sources or sinks of N_2O through denitrification and nitrification (Chapuis-Lardy et al.,
325 2007). There was a slight increase of atmospheric N_2O concentration during 1750–1860 according to the
326 ice core records, but showed a rapid increase from 1860 to present (Ciais et al., 2014). Nature sources of
327 N_2O emissions have been discussed in section 3.2 & 3.3. Previous studies found that there were some
328 anthropogenic N_2O emissions along with the natural sources in the pre-industrial era (Davidson, 2009;
329 Syakila and Kroeze, 2011). Syakila and Kroeze (2011) found anthropogenic N_2O emission began since
330 1500 because of the biomass burning and agriculture. The total anthropogenic N_2O emission in their study
331 was estimated as 1.1 Tg N in 1850. In addition, Davidson (2009) derived a time-course analysis of sources
332 and sinks of atmospheric N_2O since 1860. The pre-industrial anthropogenic N_2O sources in his study
333 included biomass burning, agriculture (e.g. manure application, and the cultivation of legume) and human
334 sewage, the sum of which was 0.7 (0.6–0.8) Tg N yr^{-1} (Davidson, 2009). Thus, anthropogenic N_2O
335 emission has already existed in 1860, but in a small magnitude as compared with the contemporary amount.

336 Davidson (2009) mentioned that there was possibly a certain amount of N_2O loss in the pre-industrial
337 period through atmospheric sink and the reduced emission from tropical deforestation. He estimated the
338 anthropogenic sink as 0.26 Tg N in 1860. In addition, the deforestation of tropical forest might have caused
339 a loss of N_2O emissions in 1860, which was estimated as 0.03 Tg N (Davidson, 2009). However, studies

have shown that the conversion of forest to pasture and cropland could increase or have no effect on N_2O emissions because the effects depended on disturbance intensity of human activities on soil conditions (van Lent et al., 2015). For instance, N_2O emissions tended to increase during the first 5–10 years after conversion and thereafter might decrease to average upland forest or low canopy forest levels in the non-fertilized croplands and pastures. In contrast, emissions were at a high level during and after fertilization in fertilized croplands (van Lent et al., 2015). Thus, more work is needed to study how forest degradation affects N_2O fluxes (Mertz et al., 2012).

3.5 Future research needs

Large uncertainty still exists in the DLEM simulation associated with the quality of input datasets and parameters applied in simulations. Although input datasets could play a significant role in the variety of the model output, it is difficult to obtain accurate datasets back to the year 1860. Average climate data from 1901 to 1930 was used to run model simulation, which could raise the uncertainty in estimating N_2O emission in 1860. The datasets of LULC, N deposition, and manure application in 1860 could introduce uncertainties to this estimate. The average oceanic and atmospheric chemistry emissions cited from the IPCC AR5 could introduce the uncertainty into calculation of the total natural emissions in 1860 when comparing with the estimate done by Prather et al. (2015). Thus, more accurate estimate of oceanic N_2O emission is significant to narrow the confidence estimate of the pre-industrial terrestrial sources. The N_2O fluxes from wetlands and peats needed to be included in the future study.

4 Conclusions

Using the process-based land ecosystem model DLEM, this study provides a spatially-explicit estimate of pre-industrial N_2O emissions for major PFTs and critical regions across global land surface. Improved LHS was performed to analyze uncertainty ranges of the estimates. We estimated that pre-industrial N_2O

emission is 6.20 Tg N yr^{-1}. The modeled results showed a large spatial variability due to variations in climate conditions and PFTs. Tropical ecosystem was the dominant contributor of global N_2O emissions. In contrast, boreal regions contributed less than 5% to the total emission. China, India and United States are top countries accounted for emissions from croplands in 1860. While uncertainties still exist in the N_2O emission estimation in the pre-industrial era, this study offered a relatively reasonable estimate of the pre-industrial N_2O emission from land soils. Meanwhile, this study provided a spatial estimate for N_2O emission from the global hot spots, which could be used as a reference to estimate net human-induced emissions in the contemporary period.

Author Contributions

Tian H., Pan, S., and Xu, R. initiated this research and designed model simulations. Xu R. performed DLEM simulations, analyses and calculations. Lu C. contributed to the model calibration and data analysis. Chen J. contributed to the data processing and statistical analysis. Yang J. took charge of input datasets preparation (environmental factors), data description, and model verification. Zhang B. provided manure N input data. All coauthors contribute manuscript development.

Acknowledgements

This work was supported by National Science Foundation (NSF) Grants (1243232, 121036), Chinese Academy of Sciences STS Program (KFJ-STS-ZDTP-010-05) and Auburn University IGP Program. We wish to thank the previous members in the Ecosystem Dynamics and Global Ecology (EDGE) Laboratory who made great contributions to the improvements and developments of the DLEM and associated geo-referenced data set in the past decade.

References

Aardenne, J. V., Dentener, F., Olivier, J., Goldewijk, C., and Lelieveld, J.: A 1× 1 resolution data set of historical anthropogenic trace gas emissions for the period 1890–1990, Global Biogeochemical Cycles, 15, 909-928, 2001.

Alexander, V., and Billington, M.: Nitrogen fixation in the Alaskan taiga, in: Forest ecosystems in the Alaskan taiga, Springer, 112-120, 1986.

Augustin, J., Merbach, W., Steffens, L., and Snelinski, B.: Nitrous oxide fluxes of disturbed minerotrophic peatlands, Agribiological Research, 51, 47-57, 1998.

Bate, G., and Gunton, C.: Nitrogen in the Burkea savanna, in: Ecology of tropical savannas, Springer, 498-513, 1982.

Bouwman, A., Fung, I., Matthews, E., and John, J.: Global analysis of the potential for N_2O production in natural soils, Global Biogeochemical Cycles, 7, 557-597, 1993.

Bouwman, A., Van der Hoek, K., and Olivier, J.: Uncertainties in the global source distribution of nitrous oxide, Journal of Geophysical Research: Atmospheres, 100, 2785-2800, 1995.

Breuer, L., Papen, H., and Butterbach-Bahl, K.: N_2O emission from tropical forest soils of Australia, Journal of Geophysical Research: Atmospheres, 105, 26353-26367, 2000.

Butterbach-Bahl, K., Gasche, R., Huber, C., Kreutzer, K., and Papen, H.: Impact of N-input by wet deposition on N-trace gas fluxes and CH_4-oxidation in spruce forest ecosystems of the temperate zone in Europe, Atmospheric Environment, 32, 559-564, 1998.

Butterbach-Bahl, K., Baggs, E. M., Dannenmann, M., Kiese, R., and Zechmeister-Boltenstern, S.: Nitrous oxide emissions from soils: how well do we understand the processes and their controls?, Phil. Trans. R. Soc. B, 368, 20130122, 2013.

Chapuis-Lardy, L., Wrage, N., Metay, A., CHOTTE, J. L., and Bernoux, M.: Soils, a sink for N2O? A review, Global Change Biology, 13, 1-17, 2007.

Chatskikh, D., Olesen, J. E., Berntsen, J., Regina, K., and Yamulki, S.: Simulation of effects of soils, climate and management on N_2O emission from grasslands, Biogeochemistry, 76, 395-419, 2005.

Chen, G. X., Huang, B., Xu, H., Zhang, Y., Huang, G., Yu, K., Hou, A., Du, R., Han, S., and VanCleemput, O.: Nitrous oxide emissions from terrestrial ecosystems in China, Chemosphere-Global Change Science, 2, 373-378, 2000.

Ciais, P., Sabine, C., Bala, G., Bopp, L., Brovkin, V., Canadell, J., Chhabra, A., DeFries, R., Galloway, J., Heimann, M. and Jones, C.: Carbon and other biogeochemical cycles. In Climate Change 2013: The Physical Science Basis. Contribution of Working Group I to the Fifth Assessment Report of the Intergovernmental Panel on Climate Change. Cambridge University Press, 465-570, 2014.

Cleveland, C. C., Townsend, A. R., Schimel, D. S., Fisher, H., Howarth, R. W., Hedin, L. O., Perakis, S. S., Latty, E. F., Von Fischer, J. C., and Elseroad, A.: Global patterns of terrestrial biological nitrogen (N_2) fixation in natural ecosystems, Global Biogeochemical Cycles, 13, 623-645, 1999.

Cleveland, C. C., Houlton, B. Z., Neill, C., Reed, S. C., Townsend, A. R., and Wang, Y.: Using indirect methods to constrain symbiotic nitrogen fixation rates: a case study from an Amazonian rain forest, Biogeochemistry, 99, 1-13, 2010.

Couwenberg, J., Thiele, A., Tanneberger, F., Augustin, J., Bärisch, S., Dubovik, D., Liashchynskaya, N., Michaelis, D., Minke, M., and Skuratovich, A.: Assessing greenhouse gas emissions from peatlands using vegetation as a proxy, Hydrobiologia, 674, 67-89, 2011.

Davidson, E. A., Ishida, F. Y., and Nepstad, D. C.: Effects of an experimental drought on soil emissions of carbon dioxide, methane, nitrous oxide, and nitric oxide in a moist tropical forest, Global Change Biology, 10, 718-730, 2004.

427 Davidson, E. A.: The contribution of manure and fertilizer nitrogen to atmospheric nitrous oxide since 1860, Nature
428 Geoscience, 2, 659-662, 2009.
429 Davidson, E. A., and Kanter, D.: Inventories and scenarios of nitrous oxide emissions, Environmental Research
430 Letters, 9, 105012, 2014.
431 Dentener, F.: Global maps of atmospheric nitrogen deposition, 1860, 1993, and 2050, Data set. Available on-line
432 (http://daac. ornl. gov/) from Oak Ridge National Laboratory Distributed Active Archive Center, Oak Ridge, TN,
433 USA, 2006.
434 Denman K., Brasseur G., Chidthaisong A., Ciais P. M., Cox P., Dickinson R., Hauglustaine D., Heinze C., Holland
435 E., Jacob D., Lohmann U., Ramachandran S., da Silva Dias P., Wofsy S. and Zhang X.: Couplings Between
436 Changes in the Climate System and Biogeochemistry. In: Climate Change 2007: The Physical Science Basis.
437 Contribution of Working Group I to the Fourth Assessment Report of the Intergovernmental Panel on Climate
438 Change [Solomon S., Qin D., Manning M., Chen Z., Marquis M., Averyt K. B., Tignor M., and Miller H. (eds.)].
439 Cambridge University Press, Cambridge, United Kingdom and New York, NY, USA, 501-566, 2007.
440 Duxbury, J., Bouldin, D., Terry, R., and Tate, R. L.: Emissions of nitrous oxide from soils, 1982.
441 Eickenscheidt, N., and Brumme, R.: NO_x and N_2O fluxes in a nitrogen-enriched European spruce forest soil under
442 experimental long-term reduction of nitrogen depositions, Atmospheric Environment, 60, 51-58, 2012.
443 Erickson, H., Keller, M., and Davidson, E. A.: Nitrogen oxide fluxes and nitrogen cycling during postagricultural
444 succession and forest fertilization in the humid tropics, Ecosystems, 4, 67-84, 2001.
445 Erickson, H. E., and Perakis, S. S.: Soil fluxes of methane, nitrous oxide, and nitric oxide from aggrading forests in
446 coastal Oregon, Soil Biology and Biochemistry, 76, 268-277, 2014.
447 Forster, P., Ramaswamy, V., Artaxo, P., Berntsen, T., Betts, R., Fahey, D. W., Haywood, J., Lean, J., Lowe, D. C.,
448 and Myhre, G.: Changes in atmospheric constituents and in radiative forcing. Chapter 2, in: Climate Change
449 2007. The Physical Science Basis, 2007.
450 Galloway, J. N., Dentener, F. J., Capone, D. G., Boyer, E. W., Howarth, R. W., Seitzinger, S. P., Asner, G. P.,
451 Cleveland, C., Green, P., and Holland, E.: Nitrogen cycles: past, present, and future, Biogeochemistry, 70, 153-
452 226, 2004.
453 Gerber, S., Hedin, L. O., Oppenheimer, M., Pacala, S. W., and Shevliakova, E.: Nitrogen cycling and feedbacks in a
454 global dynamic land model, Global Biogeochemical Cycles, 24, 2010.
455 Gerber, J. S., Carlson, K. M., Makowski, D., Mueller, N. D., Garcia de Cortazar-Atauri, I., Havlík, P., Herrero, M.,
456 Launay, M., O'Connell, C. S., and Smith, P.: Spatially explicit estimates of N_2O emissions from croplands
457 suggest climate mitigation opportunities from improved fertilizer management, Global Change Biology, 2016.
458 Goodroad, L., and Keeney, D.: Nitrous oxide emission from forest, marsh, and prairie ecosystems, Journal of
459 Environmental Quality, 13, 448-452, 1984.
460 Hadi, A., Inubushi, K., Purnomo, E., Razie, F., Yamakawa, K., and Tsuruta, H.: Effect of land-use changes on
461 nitrous oxide (N_2O) emission from tropical peatlands, Chemosphere-Global Change Science, 2, 347-358, 2000.
462 Hadi, A., Inubushi, K., Furukawa, Y., Purnomo, E., Rasmadi, M., and Tsuruta, H.: Greenhouse gas emissions from
463 tropical peatlands of Kalimantan, Indonesia, Nutrient Cycling in Agroecosystems, 71, 73-80, 2005.
464 Hall, S. J., and Matson, P. A.: Nitrogen oxide emissions after nitrogen additions in tropical forests, Nature, 400, 152-
465 155, 1999.
466 Hansen, S.: Daisy, a flexible soil-plant-atmosphere system model, Report. Dept. Agric, 2002.
467 Heinen, M.: Simplified denitrification models: overview and properties, Geoderma, 133, 444-463, 2006.
468 Hoeft, I., Steude, K., Wrage, N., and Veldkamp, E.: Response of nitrogen oxide emissions to grazer species and plant
469 species composition in temperate agricultural grassland, Agriculture, ecosystems & environment, 151, 34-43,
470 2012.

Holland, E., Lee-Taylor, J., Nevison, C., and Sulzman, J.: Global N Cycle: Fluxes and N_2O mixing ratios originating from human activity, Data set. Available on-line: http://www. daac. ornl. gov from Oak Ridge National Laboratory Distributed Active Archive Center, Oak Ridge, Tennessee, USA, doi, 10, 2005.

Holtgrieve, G. W., Jewett, P. K., and Matson, P. A.: Variations in soil N cycling and trace gas emissions in wet tropical forests, Oecologia, 146, 584-594, 2006.

Horváth, L., Führer, E., and Lajtha, K.: Nitric oxide and nitrous oxide emission from Hungarian forest soils; linked with atmospheric N-deposition, Atmospheric Environment, 40, 7786-7795, 2006.

Hu, M., Chen, D., and Dahlgren, R. A.: Modeling nitrous oxide (N_2O) emission from rivers: A global assessment, Global Change Biology, 2016.

Hurtt, G., Chini, L. P., Frolking, S., Betts, R., Feddema, J., Fischer, G., Fisk, J., Hibbard, K., Houghton, R., and Janetos, A.: Harmonization of land-use scenarios for the period 1500–2100: 600 years of global gridded annual land-use transitions, wood harvest, and resulting secondary lands, Climatic Change, 109, 117-161, 2011.

Huttunen, J. T., Alm, J., Liikanen, A., Juutinen, S., Larmola, T., Hammar, T., Silvola, J., and Martikainen, P. J.: Fluxes of methane, carbon dioxide and nitrous oxide in boreal lakes and potential anthropogenic effects on the aquatic greenhouse gas emissions, Chemosphere, 52, 609-621, 2003.

Intergovernmental Panel on Climate Change (IPCC) Revised 1996 IPCC Guidelines for National Greenhouse Gas Inventories vol 1/3 ed J T Houghton, L G Meira Filho, B Lim, K Treanton, I Mamaty, Y Bonduki, D J Griggs and B A Callander (London: IPCC, OECD and IEA), 1997.

Jung, M., Henkel, K., Herold, M., and Churkina, G.: Exploiting synergies of global land cover products for carbon cycle modeling, Remote Sensing of Environment, 101, 534-553, 2006.

Keller, M., and Reiners, W. A.: Soil-atmosphere exchange of nitrous oxide, nitric oxide, and methane under secondary succession of pasture to forest in the Atlantic lowlands of Costa Rica, Global Biogeochemical Cycles, 8, 399-409, 1994.

Kitzler, B., Zechmeister-Boltenstern, S., Holtermann, C., Skiba, U., and Butterbach-Bahl, K.: Nitrogen oxides emission from two beech forests subjected to different nitrogen loads, Biogeosciences, 3, 293-310, 2006.

Kroeze, C., Mosier, A., and Bouwman, L.: Closing the global N_2O budget: a retrospective analysis 1500–1994, Global Biogeochemical Cycles, 13, 1-8, 1999.

van Lent, J., Hergoualc'h, K., and Verchot, L.: Reviews and syntheses: Soil N_2O and NO emissions from land use and land use change in the tropics and subtropics: a meta-analysis, Biogeosciences, 12, 2015.

Liu, M., Tian, H., Yang, Q., Yang, J., Song, X., Lohrenz, S. E., and Cai, W. J.: Long-term trends in evapotranspiration and runoff over the drainage basins of the Gulf of Mexico during 1901–2008, Water Resources Research, 49, 1988-2012, 2013.

Lu, C., and Tian, H.: Net greenhouse gas balance in response to nitrogen enrichment: perspectives from a coupled biogeochemical model, Global Change Biology, 19, 571-588, 2013.

Luizão, F., Matson P., Livingston G., Luizao R. and Vitousek P.M.: Nitrous oxide flux following tropical land clearing, Global Biogeochemical Cycle, 3:281-285, 1989.

Machida, T., Nakazawa, T., Fujii, Y., Aoki, S., and Watanabe, O.: Increase in the atmospheric nitrous oxide concentration during the last 250 years, Geophysical Research Letters, 22, 2921-2924, 1995.

Martikainen, P. J., Nykänen, H., Crill, P., and Silvola, J.: Effect of a lowered water table on nitrous oxide fluxes from northern peatlands, Nature, 366, 51-53, 1993.

Mertz, O., Müller, D., Sikor, T., Hett, C., Heinimann, A., Castella, J.-C., Lestrelin, G., Ryan, C. M., Reay, D. S., Schmidt-Vogt, D., Danielsen, F., Theilade, I., Noordwijk, M. v., Verchot, L. V., Burgess, N. D., Berry, N. J., Pham, T. T., Messerli, P., Xu, J., Fensholt, R., Hostert, P., Pflugmacher, D., Bruun, T. B., Neergaard, A. d., Dons, K., Dewi, S., Rutishauser, E., Sun, and Zhanli: The forgotten D: challenges of addressing forest degradation in

complex mosaic landscapes under REDD+, Geografisk Tidsskrift-Danish Journal of Geography, 112, 63-76, 10.1080/00167223.2012.709678, 2012.
Morse, J. L., Durán, J., Beall, F., Enanga, E. M., Creed, I. F., Fernandez, I., and Groffman, P. M.: Soil denitrification fluxes from three northeastern North American forests across a range of nitrogen deposition, Oecologia, 177, 17-27, 2015.
Mosier, A., Morgan, J., King, J., Lecain, D., and Milchunas, D.: Soil-atmosphere exchange of CH_4, CO_2, NO_x, and N_2O in the Colorado shortgrass steppe under elevated CO_2, Plant and Soil, 240, 201-211, 2002.
Myhre, G., Shindell, D., Bréon, F., Collins, W., Fuglestvedt, J., Huang, J., Koch, D., Lamarque, J., Lee, D., and Mendoza, B.: Anthropogenic and natural radiative forcing, Climate Change, 423, 2013.
NOAA2006A: Combined Nitrous Oxide data from the NOAA/ESRL Global Monitoring Division, 2016.
Pan, S., Tian, H., Dangal, S. R., Zhang, C., Yang, J., Tao, B., Ouyang, Z., Wang, X., Lu, C., and Ren, W.: Complex Spatiotemporal Responses of Global Terrestrial Primary Production to Climate Change and Increasing Atmospheric CO_2 in the 21 st Century, PloS one, 9, e112810, 2014.
Pan, S., Tian, H., Dangal, S. R., Yang, Q., Yang, J., Lu, C., Tao, B., Ren, W., and Ouyang, Z.: Responses of global terrestrial evapotranspiration to climate change and increasing atmospheric CO_2 in the 21st century, Earth's Future, 3, 15-35, 2015.
Prather, M. J., and Hsu, J.: Coupling of nitrous oxide and methane by global atmospheric chemistry, Science, 330, 952-954, 2010.
Prather, M. J., Holmes, C. D., and Hsu, J.: Reactive greenhouse gas scenarios: Systematic exploration of uncertainties and the role of atmospheric chemistry, Geophysical Research Letters, 39, 2012.
Prather, M. J., Hsu, J., DeLuca, N. M., Jackman, C. H., Oman, L. D., Douglass, A. R., Fleming, E. L., Strahan, S. E., Steenrod, S. D., and Søvde, O. A.: Measuring and modeling the lifetime of nitrous oxide including its variability, Journal of Geophysical Research: Atmospheres, 120, 5693-5705, 2015.
Rahn, T., and Wahlen, M.: A reassessment of the global isotopic budget of atmospheric nitrous oxide, Global Biogeochemical Cycles, 14, 537-543, 2000.
Ravishankara, A., Daniel, J. S., and Portmann, R. W.: Nitrous oxide (N_2O): the dominant ozone-depleting substance emitted in the 21st century, Science, 326, 123-125, 2009.
Reay, D. S., Davidson, E. A., Smith, K. A., Smith, P., Melillo, J. M., Dentener, F., and Crutzen, P. J.: Global agriculture and nitrous oxide emissions, Nature Climate Change, 2, 410-416, 2012.
Ren, W., Tian, H., Xu, X., Liu, M., Lu, C., Chen, G., Melillo, J., Reilly, J., and Liu, J.: Spatial and temporal patterns of CO_2 and CH_4 fluxes in China's croplands in response to multifactor environmental changes, Tellus B, 63, 222-240, 2011.
Rochette, P., Angers, D. A., Bélanger, G., Chantigny, M. H., Prévost, D., and Lévesque, G.: Emissions of N O from Alfalfa and Soybean Crops in Eastern Canada, Soil Science Society of America Journal, 68, 493-506, 2004.
Sawamoto, T., Nakajima, Y., Kasuya, M., Tsuruta, H., and Yagi, K.: Evaluation of emission factors for indirect N_2O emission due to nitrogen leaching in agro-ecosystems, Geophysical Research Letters, 32, 2005.
Schmidt, I., van Spanning, R. J., and Jetten, M. S.: Denitrification and ammonia oxidation by Nitrosomonas europaea wild-type, and NirK-and NorB-deficient mutants, Microbiology, 150, 4107-4114, 2004.
Scholes, M., Martin, R., Scholes, R., Parsons, D., and Winstead, E.: NO and N_2O emissions from savanna soils following the first simulated rains of the season, Nutrient Cycling in Agroecosystems, 48, 115-122, 1997.
Smith, K. A., and Arah, J.: Losses of nitrogen by denitrification and emissions of nitrogen oxides from soils, Proceedings-Fertiliser Society, 1990.

Spahni, R., Chappellaz, J., Stocker, T. F., Loulergue, L., Hausammann, G., Kawamura, K., Flückiger, J., Schwander, J., Raynaud, D., and Masson-Delmotte, V.: Atmospheric methane and nitrous oxide of the late Pleistocene from Antarctic ice cores, Science, 310, 1317-1321, 2005.

Stehfest, E., and Bouwman, L.: N_2O and NO emission from agricultural fields and soils under natural vegetation: summarizing available measurement data and modeling of global annual emissions, Nutrient Cycling in Agroecosystems, 74, 207-228, 2006.

Syakila, A., and Kroeze, C.: The global nitrous oxide budget revisited, Greenhouse Gas Measurement and Management, 1, 17-26, 2011.

Thompson, R. L., Ishijima, K., Saikawa, E., Corazza, M., Karstens, U., Patra, P. K., Bergamaschi, P., Chevallier, F., Dlugokencky, E., and Prinn, R. G.: TransCom N_2O model inter-comparison–Part 2: Atmospheric inversion estimates of N_2O emissions, Atmospheric chemistry and physics, 14, 6177-6194, 2014.

Tian, H., Xu, X., Liu, M., Ren, W., Zhang, C., Chen, G., and Lu, C.: Spatial and temporal patterns of CH_4 and N_2O fluxes in terrestrial ecosystems of North America during 1979–2008: application of a global biogeochemistry model, Biogeosciences, 7, 2673-2694, 2010.

Tian, H., Xu, X., Lu, C., Liu, M., Ren, W., Chen, G., Melillo, J., and Liu, J.: Net exchanges of CO_2, CH_4, and N_2O between China's terrestrial ecosystems and the atmosphere and their contributions to global climate warming, Journal of Geophysical Research: Biogeosciences, 116, 2011.

Tian, H., Chen, G., Zhang, C., Liu, M., Sun, G., Chappelka, A., Ren, W., Xu, X., Lu, C., and Pan, S.: Century-scale responses of ecosystem carbon storage and flux to multiple environmental changes in the southern United States, Ecosystems, 15, 674-694, 2012.

Tian, H., Chen, G., Lu, C., Xu, X., Ren, W., Zhang, B., Banger, K., Tao, B., Pan, S., and Liu, M.: Global methane and nitrous oxide emissions from terrestrial ecosystems due to multiple environmental changes, Ecosystem Health and Sustainability, 1, 1-20, 2015.

Tian, H., Lu, C., Ciais, P., Michalak, A. M., Canadell, J. G., Saikawa, E., Huntzinger, D. N., Gurney, K. R., Sitch, S., and Zhang, B., J. Yang, P. Bousquet, L. Bruhwiler, G. Chen, E. Dlugokencky, P. Friedlingstein, J. Melillo, S. Pan, B. Poulter, R. Prinn, M. Saunois, C.R. Schwalm, S.C. Wofsy: The terrestrial biosphere as a net source of greenhouse gases to the atmosphere, Nature, 531, 225-228, 2016.

Vitousek, P. M., Menge, D. N., Reed, S. C., and Cleveland, C. C.: Biological nitrogen fixation: rates, patterns and ecological controls in terrestrial ecosystems, Philosophical Transactions of the Royal Society of London B: Biological Sciences, 368, 20130119, 2013.

Volk, C., Elkins, J., Fahey, D., Dutton, G., Gilligan, J., Loewenstein, M., Podolske, J., Chan, K., and Gunson, M.: Evaluation of source gas lifetimes from stratospheric observations, Journal of Geophysical Research: Atmospheres, 102, 25543-25564, 1997.

Wei, Y., Liu, S., Huntzinger, D. N., Michalak, A., Viovy, N., Post, W., Schwalm, C. R., Schaefer, K., Jacobson, A., and Lu, C.: The North American Carbon Program Multi-scale Synthesis and Terrestrial Model Intercomparison Project–Part 2: Environmental driver data, Geoscientific Model Development, 7, 2875-2893, 2014.

Sun, X. Y., and Xu, H. C.: Emission flux of nitrous oxide from forest soils in Beijing, Scientia Silvae Sinicae, 37, 57-63, 2001.

Werner, C., Butterbach-Bahl, K., Haas, E., Hickler, T., and Kiese, R.: A global inventory of N_2O emissions from tropical rainforest soils using a detailed biogeochemical model, Global Biogeochemical Cycles, 21, 2007.

Wrage, N., Velthof, G., Van Beusichem, M., and Oenema, O.: Role of nitrifier denitrification in the production of nitrous oxide, Soil biology and Biochemistry, 33, 1723-1732, 2001.

Xu, X., H. Tian, M. Liu, W. Ren, G. Chen and C. Lu and C. Zhang. Multiple-factor controls on terrestrial N_2O flux over North America. *Biogeosciences* 9, 1351-1366, 2012.

Yang, Q., Tian, H., Friedrichs, M. A., Hopkinson, C. S., Lu, C., and Najjar, R. G.: Increased nitrogen export from eastern North America to the Atlantic Ocean due to climatic and anthropogenic changes during 1901–2008, Journal of Geophysical Research: Biogeosciences, 120, 1046-1068, 2015.

Zhang, B., Tian, H., Lu, C., Dangal, S. R. S., Yang, J., and Pan, S.: Manure nitrogen production and application in cropland and rangeland during 1860–2014: A 5-minute gridded global data set for Earth system modeling, Earth System Science Data Discussion, in review, 2017.

Zhang, B., Tian, H., Ren, W., Tao, B., Lu, C., Yang, J., Banger, K., and Pan, S.: Methane emissions from global rice fields: Magnitude, spatiotemporal patterns, and environmental controls, Global Biogeochemical Cycles, 2016.

Zhuang, Q., Lu, Y., and Chen, M.: An inventory of global N_2O emissions from the soils of natural terrestrial ecosystems, Atmospheric Environment, 47, 66-75, 2012.

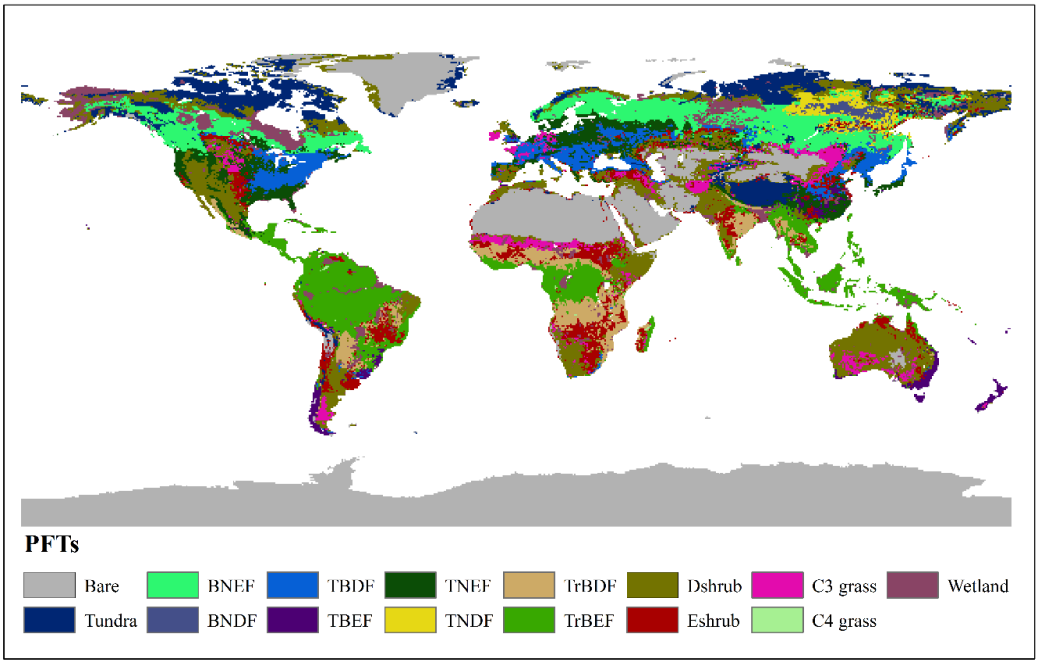

Fig. 1 Global potential natural vegetation map in the pre-industrial era used by DLEM. BNEF: Boreal Needleleaf Evergreen Forest, BNDF: Boreal Needleleaf Deciduous Forest, TBDF: Temperate Broadleaf Deciduous Forest, TBEF: Temperate Broadleaf Evergreen Forest, TNEF: Temperate Needleleaf Evergreen Forest, TNDF: Temperate Needleleaf Deciduous Forest, TrBDF: Tropical Broadleaf Deciduous Forest, TrBEF: Tropical Broadleaf Evergreen Forest, Dshrub: Decidous Shrubland, Eshrub: Evergreen Shrubland.

618

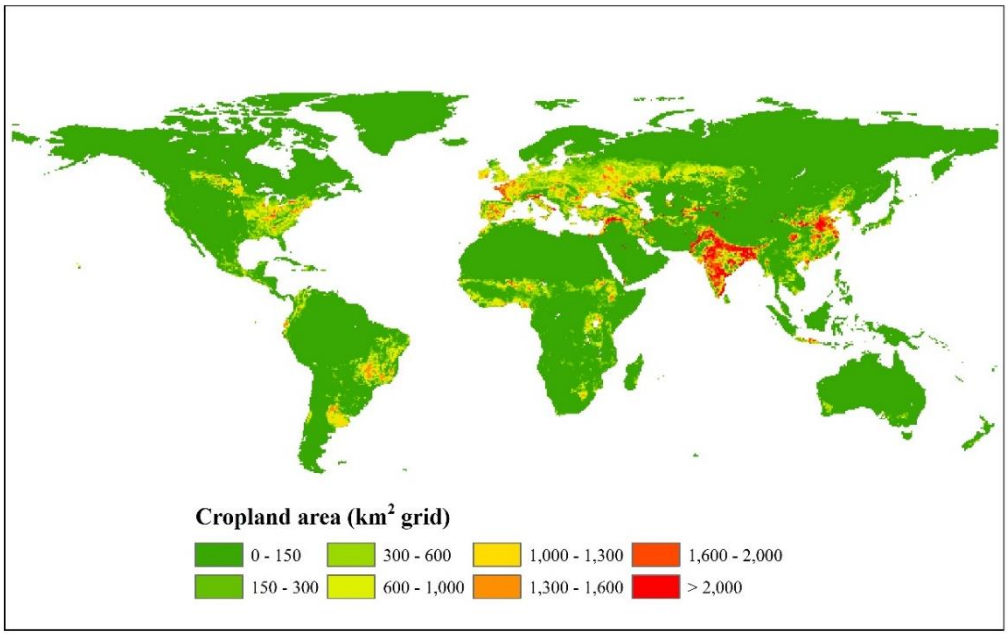

619

620 **Fig. 2** The spatial distribution of cropland area in the year1860.

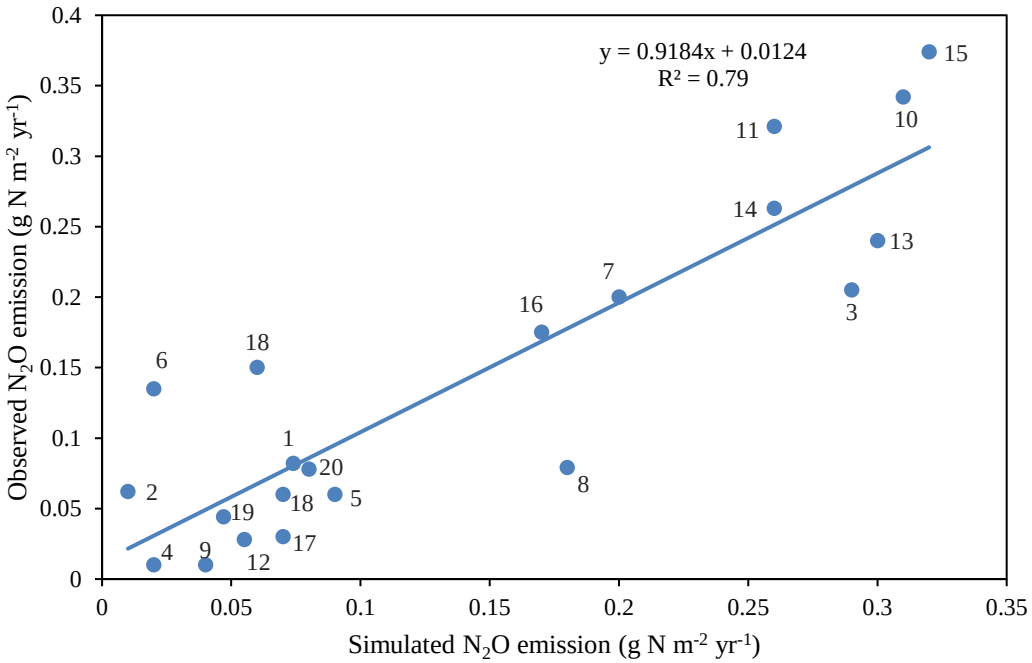

Fig. 3 The comparison of the DLEM-simulated N_2O emissions with field observations. All sites were described in the supplementary material (Table S1).

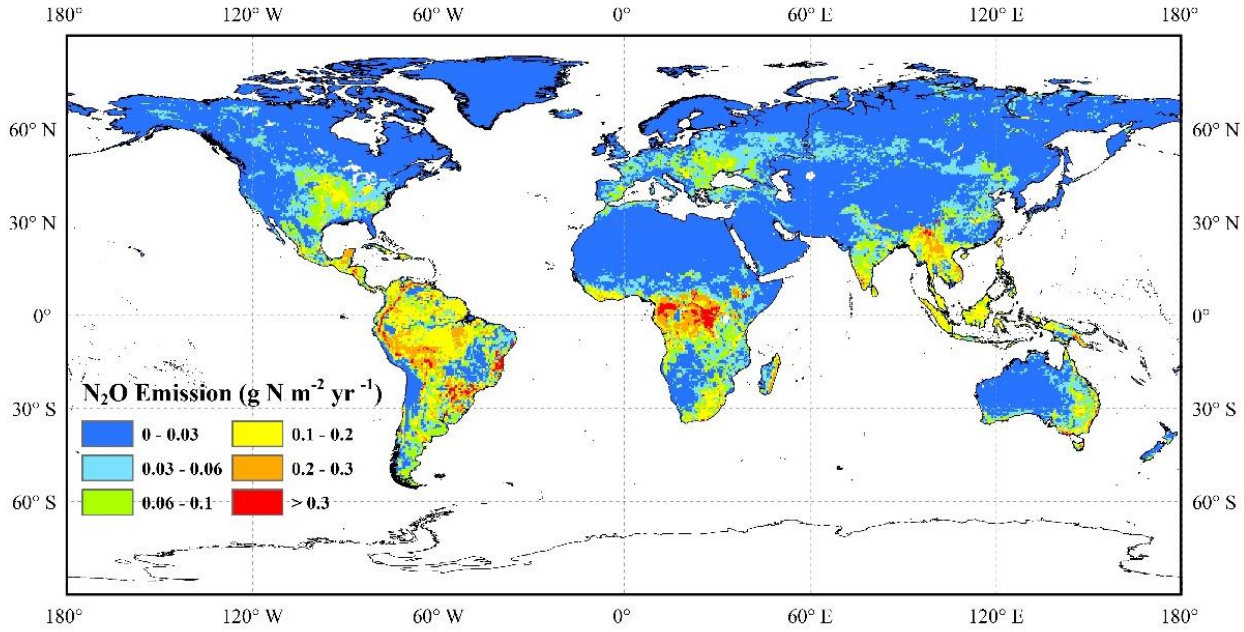

Fig. 4 The spatial distribution of N_2O emission in the pre-industrial era.

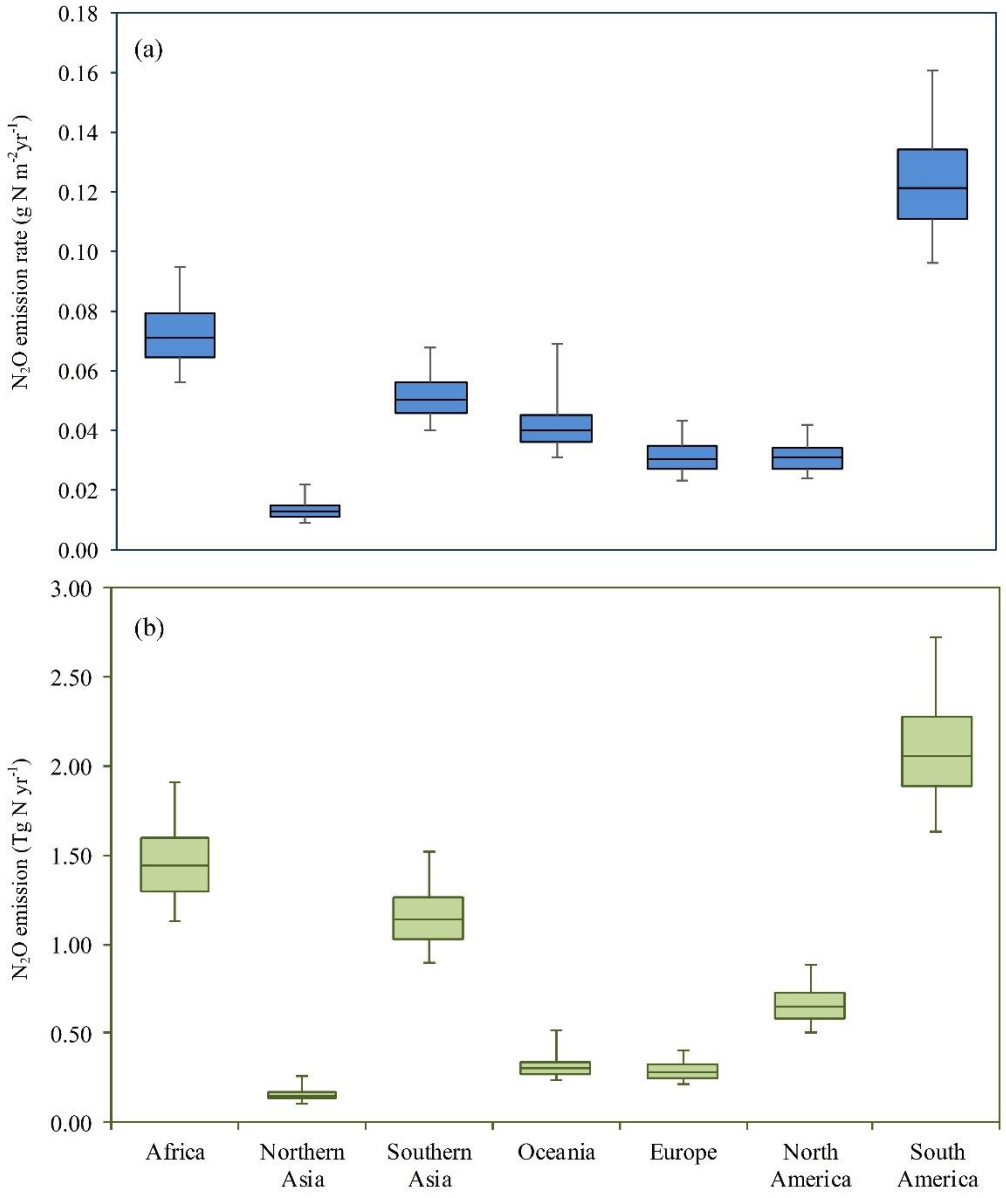

630

631 **Fig. 5** Estimated N_2O emission rates (a) and emissions (b) with uncertainty ranges at continental-level in the year 1860. Solid
632 line within each box refers to the median value of N_2O emission rate or amount.

633

634

635

636

637

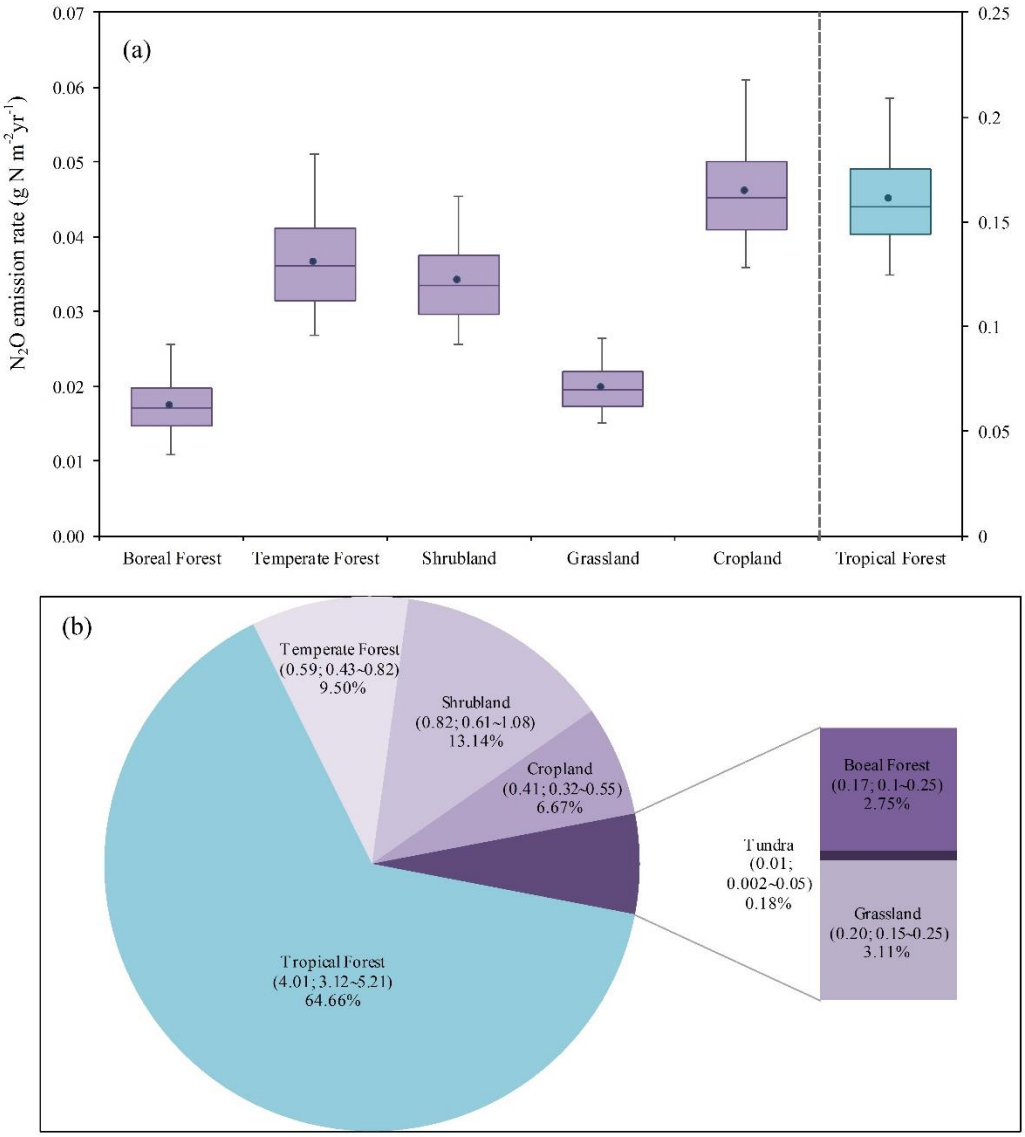

638

639 **Fig. 6** (a) Estimated N_2O emission rate at biome-level in the year 1860 with the median value (solid line), the mean (solid dot),
640 and the uncertainty range of emission rates from different biomes. The emission rate in the tundra was removed because of the
641 extremely small value (less than 0.003g N $m^{-2}yr^{-1}$); (b) Estimated N_2O emission (Tg N yr^{-1}) with uncertainty ranges and its
642 percentage (%) at biome-level in the year 1860.

643

644

645

646

647

Table 1. Pre-industrial N_2O emissions from natural vegetation and croplands in different countries. 1Mha = 10^4 km^2

Country	Vegetation area (Mha)	Natural soils (Gg N yr^{-1})	Cropland (Gg N yr^{-1})	Total (Gg N yr^{-1})
China	756.3	188	62	250
India	306.8	121	64	185
United States	913.9	296	81	377
Pakistan	65.1	5	6	11
Indonesia	174.1	181	2	183
France	52.3	7	9	16
Brazil	835.1	1017	11	1028
Canada	914.6	94	2	96
Germany	36.0	9	4	13
Turkey	74.3	17	11	28
Mexico	191.0	118	3	121
Vietnam	31.7	41	2	43
Spain	48.2	14	6	20
Russian Federation	1575.3	234	19	253
Bangladesh	12.4	2	5	7
Thailand	49.3	56	3	59